Hindawi
Complexity
Volume 2019, Article ID 3879626, 16 pages
https://doi.org/10.1155/2019/3879626

Research Article

Dynamics Induced by Delay in a Nutrient-Phytoplankton Model with Multiple Delays

Chuanjun Dai,[1,2] Hengguo Yu ,[3] Qing Guo,[4] He Liu,[4] Qi Wang,[1,2] Zengling Ma,[1,2] and Min Zhao [1,2]

[1] *Zhejiang Provincial Key Laboratory for Water Environment and Marine Biological Resources Protection, Wenzhou University, Wenzhou, Zhejiang, 325035, China*
[2] *College of Life and Environmental Science, Wenzhou University, Wenzhou, Zhejiang, 325035, China*
[3] *College of Mathematics, Physics and Electronic Information Engineering, Wenzhou University, Wenzhou, Zhejiang, 325035, China*
[4] *Environmental Engineering Program, University of Northern British Columbia, Prince George, British Columbia, V2N 4Z9, Canada*

Correspondence should be addressed to Min Zhao; zmcn@tom.com

Received 5 October 2018; Revised 11 December 2018; Accepted 9 January 2019; Published 3 February 2019

Guest Editor: Baltazar Aguirre-Hernandez

A nutrient-phytoplankton model with multiple delays is studied analytically and numerically. The aim of this paper is to study how the delay factors influence dynamics of interaction between nutrient and phytoplankton. The analytical analysis indicates that the positive equilibrium is always globally asymptotically stable when the delay does not exist. On the contrary, the positive equilibrium loses its stability via Hopf instability induced by delay and then the corresponding periodic solutions emerge. Especially, the stability switches for positive equilibrium occur as the delay is increased. Furthermore, the numerical simulations show that periodic-2 and periodic-3 solutions can appear due to the existence of delays. Numerical results are consistent with the analytical results. Our results demonstrate that the delay has a great impact on the nutrient-phytoplankton dynamics.

1. Introduction

Some phytoplankton, for example, Cyanobacteria, can form dense and sometimes toxic blooms in freshwater and marine environments, which threaten ecological balance, drinking water, fisheries, and even human health [1]. However, the mechanism, by which phytoplankton blooms occur, is currently not very clear, which contribute to the difficulty to prevent or mitigate the proliferation of phytoplankton blooms. These have stimulated lots of researches aiming to understand the growth mechanisms of phytoplankton.

In recent years, dynamics in phytoplankton growth have drawn increasing attention from experimental ecologists, as well as mathematical ecologists. Some results from experiments and field observations imply that many factors affecting the dynamics of phytoplankton growth are bound to exist, such as nutrient [2], light [3], temperature [4], iron supply [5], zooplankton [6]. Especially, due to the effects of limiting factors including temperature, light, and day length, it has been indicated by Rhee and Gotham [7] that the population dynamics of phytoplankton in aquatic environments can change with season, latitude, and depth. Among factors affecting phytoplankton growth, nutrient has been an essential element [8–10], mainly including nitrogen and phosphate. Results reported by Ryther [11] indicated that phytoplankton indeed consumes lots of nitrogen and phosphate in their growth process, but reducing the nitrogen content in aquatic cannot slow the eutrophication. Using data from 17 lakes, Smith [8] analysed the influence of ratio of total nitrogen to phosphorus on the growth of blue-green algae (Cyanophya) and showed that controlling the ratio can help us improve the quality of aquatic environment very well. Obviously, the production process of phytoplankton is more complex.

However, due to the complexity and nonlinearity of aquatic ecosystem, there are some difficulties in understanding nutrient-phytoplankton dynamics only depending on experiment or field observation, which makes it necessary to use models to provide quantitative insights into dynamic mechanism of phytoplankton growth. For different aquatic environments, we can use various modifications of the classical prey-predator models by introducing functional responses to model nutrient-phytoplankton dynamics [12–14]. For example, Huppert et al. [15] describe the dynamics of nutrient-driven phytoplankton blooms by a simple model and identify, using the model analysis, an important threshold effect that a bloom will only be triggered when nutrients exceed a certain defined level. Additionally, most nutrient-phytoplankton models reveal that phytoplankton population and nutrient population can coexist at equilibrium globally under some conditions [16, 17]. However, Sherratt and Smith [18] have reported that a constant population density may not exist in reality because of the existence of some factors, such as noise and physical factors. Actually, experiments and field observations show that the changes of phytoplankton population density usually possess oscillatory behaviour [19, 20].

For the single cell phytoplankton species, in most studies of nutrient-phytoplankton models, it is usually assumed that the processes, such as conversion process of nutrient, in the dynamics of phytoplankton growth are instantaneous [14–17, 19–23]. It may be doubtful whether there exists the delay in the growth of phytoplankton over the large area or not. Yet, J. Caperon [24] studied time lag in population growth response of *Isochrysis galbana*, a phytoplankton species, to a variable nitrate environment by both experiments and model, and demonstrated the existence of delay in the growth of *Isochrysis galbana*. Hence, the delay may indeed exist in the phytoplankton growth, which means that it is necessary to consider delay in nutrient-phytoplankton models. An approach that has been attempted by researchers to model the dynamics of phytoplankton is the role of delay since delay appears as an important component in biosystems and ecosystems [25–30].

Actually, growing evidence shows that there exists time lag in some conversion processes from one state to another in some systems, and delay is an important factor because it can affect the dynamics of these systems. Volterra [31] considered time delay in a prey-predator model first and found oscillatory behaviour for the spatial distribution. For a long time, it has been recognized that delays can give rise to destabilizing effect of the dynamics of systems, where periodic solutions, as well as chaos, may emerge [32–35]. Models incorporating delays in diverse biological and ecological models are extensively studied [36–42]. Especially, the characteristic equation with respect to the linearized system of delay differential equations plays a key role in dynamic analysis, by which we can obtain some information on the stability of equilibrium. In addition, using the normal form theory, one can carry out the bifurcation analysis, such as the direction and stability of periodic solutions arising through Hopf bifurcation [43, 44].

The main purpose of this paper is to consider the effects of multiple delays on the nutrient-phytoplankton dynamics. In [15], Huppert et al. presented a simple model to investigate effect of nutrient on phytoplankton blooms, and much better results are obtained. Here, this model is extended into a "two preys-one predator" type to describe nitrogen- phosphorus-phytoplankton dynamics, as follows:

$$\begin{aligned}\frac{dN}{dt} &= I_1 - q_1N - \alpha_1 NA\\ \frac{dP}{dt} &= I_2 - q_2P - \alpha_2 PA\\ \frac{dA}{dt} &= \beta_1\alpha_1 N\left(t-\tau_1\right)A + \beta_2\alpha_2 P\left(t-\tau_2\right)A - mA\end{aligned} \quad (1)$$

where N, P, and A represent nitrogen, phosphorus, and phytoplankton population density at time t, respectively; I_1 is the nitrogen nutrients input flowing into the system and I_2 is the phosphorus nutrients input flowing into the system; q_1 is the loss rate of the nitrogen nutrients, and q_2 is the loss rate of the phosphorus nutrients; α_1 is nitrogen nutrient uptake rate of phytoplankton, and α_2 is phosphorus nutrient uptake rate of phytoplankton; β_1 and β_2 denote the efficiency of nutrient utilization; τ_1 and τ_2 are time delay parameters; m is the mortality rate of phytoplankton. Although the function, which describes nutrient uptake dynamics, is not a Michaelis-Menten function, but Lotka-Volterra type, Huppert et al. [15] have indicated that the Lotka-Volterra term is a good first approximation to the Michaelis-Menten type. From biological viewpoint, all parameters are nonnegative. $N(t)$, $P(t)$, and $A(t) \geq 0$ are continuous on $-\tau \leq t < 0$, where $\tau = \max(\tau_1, \tau_2)$ and $N(0)$, $P(0)$, and $A(0) > 0$.

The paper is organized as follows. In Section 2, we analyze the existence and stability of positive equilibrium in model (1) without delays. In Section 3, we discuss stability of positive equilibrium and Hopf bifurcation under five different cases for delay effect. Subsequently, the direction of bifurcation and the stability of periodic solutions arising through Hopf bifurcation are given in Section 4. In order to analyze further how delay effects influence nutrient-phytoplankton dynamics, a series of numerical simulations are carried out in Section 5. Finally, the paper ends with conclusion in Section 6.

2. Existence and Stability of Positive Equilibrium in Model (1) without Delays

In this section, it is presented first that the first octant is positive invariant in model (1) without delays and the following lemma holds.

Lemma 1. *All the solutions of model (1) with initial conditions that initiate in $\{R_+^3\}$ are positive invariant in the absence of delays.*

Proof. From the first equation of model (1), we have

$$\frac{dN}{dt} = I_1 - q_1N - \alpha_1 NA \geq -\left(q_1 + \alpha_1 A\right)N. \quad (2)$$

Hence, $N(t) \geq N(0)\exp[-\int_0^t (q_1+\alpha_1 A)ds] > 0$ under $N(0) > 0$.

Likewise, from the second equation of model (1), we have $P(t) \geq P(0)\exp[-\int_0^t (q_2+\alpha_2 A)ds] > 0$ under $P(0) > 0$.

In the absence of delays in model (1), from the third equation of model (1), if $A(0) > 0$, it can be obtained that

$$A(t) = A(0)\exp\left[\int_0^t (\beta_1\alpha_1 N + \beta_2\alpha_2 P - m)\,ds\right] > 0 \quad (3)$$

Obviously, all the solutions of model (1) without delays are positive invariant if the initial conditions initiate in $\{R_+^3\}$.

Then, we complete the proof. □

For model (1), it is obvious that the extinction equilibrium, $(I_1/q_1, I_2/q_2, 0)$, exists. Moreover, in order to discuss the existence of positive equilibrium, the following function is defined:

$$\begin{aligned} f(x) &= \alpha_1\alpha_2 m x^2 \\ &\quad + \left[(mq_1 - \alpha_1\beta_1 I_1)\alpha_2 + (mq_2 - \alpha_2\beta_2 I_2)\alpha_1\right]x \\ &\quad + (mq_1q_2 - \beta_1\alpha_1 I_1 q_2 - \beta_2\alpha_2 I_2 q_1), \end{aligned} \quad (4)$$

and then we can obtain

$$\begin{aligned} N^* &= \frac{I_1}{q_1 + \alpha_1 A^*}, \\ P^* &= \frac{I_2}{q_2 + \alpha_2 A^*}, \end{aligned} \quad (5)$$

where A^* is the positive root of (4).

For the function $f(x)$, we have $f(0) = 0$ when the condition, $m = (\beta_1\alpha_1 I_1/q_1) + (\beta_2\alpha_2 I_2/q_2)$, holds, and then there is no positive equilibrium in model (1). Obviously, $f(0) < 0$ holds if $m < (\beta_1\alpha_1 I_1/q_1) + (\beta_2\alpha_2 I_2/q_2)$, and then there exists a unique positive root with respect to $f(x) = 0$, which means that there exists a unique positive equilibrium in model (1) under this condition. However, when $m > (\beta_1\alpha_1 I_1/q_1) + (\beta_2\alpha_2 I_2/q_2)$, it can be verified directly that $f(0) > 0$ and $(mq_1 - \alpha_1\beta_1 I_1)\alpha_2 + (mq_2 - \alpha_2\beta_2 I_2)\alpha_1 > 0$, which implies that there is no positive equilibrium in model (1). Thus, summarizing these results, the following theorem can be obtained.

Theorem 2. *If $0 < m < (\beta_1\alpha_1 I_1/q_1) + (\beta_2\alpha_2 I_2/q_2)$ holds, then there exists a unique positive equilibrium in model (1); otherwise, there is no positive equilibrium in model (1) if $m \geq (\beta_1\alpha_1 I_1/q_1) + (\beta_2\alpha_2 I_2/q_2)$ holds.*

Letting the unique positive equilibrium be $E_* = (N^*, P^*, A^*)$, then the following theorem holds for model (1) without delays.

Theorem 3. *If the unique positive equilibrium exists in model (1) without delays, then it is globally asymptotically stable.*

Proof. We construct a Lyapunov function, as follows:

$$\begin{aligned} V &= \beta_1 \int_{N^*}^{N} \frac{s - N^*}{s}ds + \beta_2 \int_{P^*}^{P} \frac{s - P^*}{s}ds \\ &\quad + \int_{A^*}^{A} \frac{s - A^*}{s}ds \end{aligned} \quad (6)$$

In the model (1) without delays,

$$\begin{aligned} \frac{dV}{dt} &= \beta_1 \frac{N - N^*}{N}\frac{dN}{dt} + \beta_2 \frac{P - P^*}{P}\frac{dP}{dt} + \frac{A - A^*}{A}\frac{dA}{dt} \\ &= \beta_1 \frac{N - N^*}{N}(I_1 - q_1 N - \alpha_1 NA) + \beta_2 \frac{P - P^*}{P}(I_2 \\ &\quad - q_2 P - \alpha_2 PA) + \frac{A - A^*}{A}(\beta_1\alpha_1 NA + \beta_2\alpha_2 PA \\ &\quad - mA) = \beta_1 \frac{N - N^*}{N}((q_1 N^* + \alpha_1 N^* A^*) \\ &\quad - (q_1 N + \alpha_1 NA)) + \beta_2 \frac{P - P^*}{P}((q_2 P^* + \alpha_2 P^* A^*) \\ &\quad - (q_2 P + \alpha_2 PA)) + \frac{A - A^*}{A}(\beta_1\alpha_1 NA + \beta_2\alpha_2 PA \\ &\quad - (\beta_1\alpha_1 N^* + \beta_2\alpha_2 P^*)A) = -\beta_1(q_1 + \alpha_1 A^*) \\ &\quad \cdot \frac{(N - N^*)^2}{N} - \beta_2(q_2 + \alpha_2 A^*)\frac{(P - P^*)^2}{P} \end{aligned} \quad (7)$$

Obviously, $dV/dt \leq 0$ holds under existence of positive equilibrium and $dV/dt = 0$ holds if and only if $N = N^*$ and $P = P^*$. The largest invariant subset of the set of the point where $dV/dt = 0$ is $E_* = (N^*, P^*, A^*)$. Therefore, according to LaSalle's theorem, $E_* = (N^*, P^*, A^*)$ is globally asymptotically stable.

Then, we complete the proof. □

Letting the extinction equilibrium be $E_0 = (N_0, P_0, 0) = (I_1/q_1, I_2/q_2, 0)$, then we can obtain the following theorem in model (1) in the absence of delay.

Theorem 4. *In the absence of delays, let $m^* = (\beta_1\alpha_1 I_1/q_1) + (\beta_2\alpha_2 I_2/q_2)$, so that*

(i) *if $m > m^*$, then the extinction equilibrium E_0 is locally asymptotically stable;*

(ii) *if $m < m^*$, then the extinction equilibrium E_0 is unstable;*

(iii) *if $m = m^*$, then the model (1) undergoes transcritical bifurcation at the extinction equilibrium E_0.*

Proof. For simplicity, let

$$f_w(X, m) = \begin{pmatrix} I_1 - q_1 N - \alpha_1 NA \\ I_2 - q_2 P - \alpha_2 PA \\ \beta_1\alpha_1 NA + \beta_2\alpha_2 PA - mA \end{pmatrix} \quad (8)$$

and $X = [N, P, A]^T$.

The Jacobian matrix at E_0 is

$$J(E_0) = \begin{pmatrix} -q_1 & 0 & -\dfrac{\alpha_1 I_1}{q_1} \\ 0 & -q_2 & -\dfrac{\alpha_2 I_2}{q_2} \\ 0 & 0 & -(m - m^*) \end{pmatrix}. \quad (9)$$

The eigenvalues are $-q_1, -q_2, -(\mathrm{m} - m^*)$.

Obviously, if $m > m^*$, then the extinction equilibrium E_0 is locally asymptotically stable.

If $m < m^*$, then the extinction equilibrium E_0 is unstable. When $m = m^*$, the Jacobian matrix at E_0 is

$$J(E_0) = \begin{pmatrix} -q_1 & 0 & -\dfrac{\alpha_1 I_1}{q_1} \\ 0 & -q_2 & -\dfrac{\alpha_2 I_2}{q_2} \\ 0 & 0 & 0 \end{pmatrix}. \tag{10}$$

Then $J(E_0)$ has a geometrically simple zero eigenvalue with right eigenvector $\Phi = (\alpha_1 I_1 q_2^2, \alpha_2 I_2 q_1^2, -q_1^2 q_2^2)^T$ and left eigenvector $\Psi = (0, 0, 1)$.

Now

$$D_m f_w = \begin{pmatrix} 0 \\ 0 \\ -A \end{pmatrix} \tag{11}$$

and

$$\begin{aligned} &(\Psi (D_X D_m f_w) \Phi)_{E_0} = q_1^2 q_2^2 \neq 0, \\ &\Psi ((D_{XX} f_w)(\Phi, \Phi)) \\ &\quad = \left(\Psi \sum_{i=1}^{3} \left(e_i \Phi^T D_X (D_X f_i)^T \Phi \right) \right)_{E_0} \\ &\quad = -2 q_1^2 q_2^2 \left(\beta_1 I_1 \alpha_1^2 q_2^2 + \beta_2 I_2 \alpha_2^2 q_1^2 \right) \neq 0 \end{aligned} \tag{12}$$

According to [45], the model (1) undergoes transcritical bifurcation at the extinction equilibrium E_0 in the absence of delays.

Then, we complete the proof. □

Actually, when $m > m^*$ holds, the positive equilibrium does not exist, and the extinction equilibrium E_0 is globally asymptotically stable. Then, the following theorem holds.

Theorem 5. *If $m > (\beta_1 \alpha_1 I_1 / q_1) + (\beta_2 \alpha_2 I_2 / q_2)$ holds, then the extinction equilibrium $E_0 = (N_0, P_0, 0) = (I_1/q_1, I_2/q_2, 0)$ is globally asymptotically stable.*

Proof. We construct a Lyapunov function, as follows:

$$V = \beta_1 \int_{N_0}^{N} \frac{s - N_0}{s} ds + \beta_2 \int_{P_0}^{P} \frac{s - P_0}{s} ds + A \tag{13}$$

In the model (1) without delays,

$$\begin{aligned} \frac{dV}{dt} &= \beta_1 \frac{N - N_0}{N} \frac{dN}{dt} + \beta_2 \frac{P - P_0}{P} \frac{dP}{dt} + \frac{dA}{dt} \\ &= \beta_1 \frac{N - N_0}{N} (I_1 - q_1 N - \alpha_1 NA) \\ &\quad + \beta_2 \frac{P - P_0}{P} (I_2 - q_2 P - \alpha_2 PA) \\ &\quad + (\beta_1 \alpha_1 NA + \beta_2 \alpha_2 PA - mA) \\ &= \beta_1 \frac{N - N_0}{N} (q_1 N_0 - q_1 N - \alpha_1 NA) \\ &\quad + \beta_2 \frac{P - P_0}{P} (q_2 P_0 - q_2 P - \alpha_2 PA) \\ &\quad + (\beta_1 \alpha_1 NA + \beta_2 \alpha_2 PA - mA) \\ &= -\beta_1 q_1 \frac{(N - N_0)^2}{N} - \beta_2 q_2 \frac{(P - P_0)^2}{P} \\ &\quad + (\beta_1 \alpha_1 N_0 + \beta_2 \alpha_2 P_0 - m) A \\ &= -\beta_1 q_1 \frac{(N - N_0)^2}{N} - \beta_2 q_2 \frac{(P - P_0)^2}{P} \\ &\quad + \left(\frac{\beta_1 \alpha_1 I_1}{q_1} + \frac{\beta_2 \alpha_2 I_2}{q_2} - m \right) A \end{aligned} \tag{14}$$

Obviously, $dV/dt < 0$ holds if $m > (\beta_1 \alpha_1 I_1 / q_1) + (\beta_2 \alpha_2 I_2 / q_2)$. Therefore, the extinction equilibrium $E_0 = (N_0, P_0, 0) = (I_1/q_1, I_2/q_2, 0)$ is globally asymptotically stable when $m > (\beta_1 \alpha_1 I_1 / q_1) + (\beta_2 \alpha_2 I_2 / q_2)$.

Then, we complete the proof. □

3. Local Stability Analysis and the Hopf Bifurcation

In this section, we first state the following positive invariant theorem.

Lemma 6. *All the solutions of model (1) with initial conditions that initiate in $\{R_+^3\}$ are positive invariant.*

Proof. We consider (N, P, A) a noncontinuable solution of model (1); see [46], defined on $[-\tau, B)$, where $B \in (0, +\infty]$. Then we can use the method from [47] to prove that, for all $t \in [0, B)$, $N(t) > 0$, $P(t) > 0$, and $A(t) > 0$. Suppose that is not true. Then, there exists $0 < T < B$ such that, for all $t \in [0, T)$, $N(t) > 0$, $P(t) > 0$, and $A(t) > 0$ and either $N(T) = 0$, $P(T) = 0$, or $A(T) = 0$. According to Lemma 1, for all $t \in [0, T)$, we have

$$\begin{aligned} N(t) &> N(0) \exp \left[-\int_0^t (q_1 + \alpha_1 A) \, ds \right], \\ P(t) &> P(0) \exp \left[-\int_0^t (q_2 + \alpha_2 A) \, ds \right], \end{aligned} \tag{15}$$

and

$$\begin{aligned} A(t) &= A(0) \\ &\quad \cdot \exp \left[\int_0^t (\beta_1 \alpha_1 N(s - \tau_1) + \beta_2 \alpha_2 P(s - \tau_2) - m) \, ds \right]. \end{aligned} \tag{16}$$

As (N, P, A) is defined and continuous on $[-\tau, T]$, there is a $M \geq 0$ such that, for all $t \in [-\tau, T)$,

$$\begin{aligned} N(t) &> N(0)\exp\left[-\int_0^t (q_1+\alpha_1 A)\,ds\right] \\ &\geq N(0)\exp(-TM), \\ P(t) &> P(0)\exp\left[-\int_0^t (q_2+\alpha_2 A)\,ds\right] \\ &\geq P(0)\exp(-TM) \end{aligned} \tag{17}$$

and

$$\begin{aligned} A(t) &= A(0) \\ &\cdot \exp\left[\int_0^t \left(\beta_1\alpha_1 N(s-\tau_1)+\beta_2\alpha_2 P(s-\tau_2)-m\right)ds\right] \\ &\geq A(0)\exp(-TM). \end{aligned} \tag{18}$$

Taking the limit, as $t \longrightarrow T$, we can get

$$\begin{aligned} N(T) &\geq N(0)\exp(-TM) > 0, \\ P(T) &\geq P(0)\exp(-TM) > 0 \end{aligned} \tag{19}$$

and

$$A(T) \geq A(0)\exp(-TM) > 0, \tag{20}$$

which contradicts the fact that either $N(T) = 0$, $P(T) = 0$, or $A(T) = 0$. Thus, for all $t \in [0, B)$, $N(t) > 0$, $P(t) > 0$, and $A(t) > 0$.

Therefore, all the solutions of model (1) are positive invariant if the initial conditions initiate in $\{R_+^3\}$.

Then, we complete the proof. □

Next, we will discuss the stability of the unique positive equilibrium and existence of Hopf bifurcation in model (1) for five different cases: $\tau_1 > 0, \tau_2 = 0$; $\tau_1 = 0, \tau_2 > 0$; $\tau_1 = \tau_2 = \tau$; $\tau_1 \in (0, \tau_{10}), \tau_2 > 0$; $\tau_1 > 0, \tau_2 \in (0, \tau_{20})$.

According to Theorem 2, let $u_1 = N(t) - N^*$, $u_2 = P(t) - P^*$, $u_3 = A(t) - A^*$; the linearized form of model (1) can be obtained as follows:

$$\begin{aligned} \dot{u}_1 &= a_{11}u_1(t) + a_{13}u_3(t) \\ \dot{u}_2 &= a_{22}u_2(t) + a_{23}u_3(t) \\ \dot{u}_3 &= a_{31}u_1(t-\tau_1) + a_{32}u_2(t-\tau_2) \end{aligned} \tag{21}$$

where

$$\begin{aligned} a_{11} &= -q_1 - \alpha_1 A^*; \\ a_{13} &= -\alpha_1 N^*; \\ a_{22} &= -q_2 - \alpha_2 A^*; \\ a_{23} &= -\alpha_2 P^*; \\ a_{31} &= \beta_1\alpha_1 A^*; \\ a_{32} &= \beta_2\alpha_2 A^*. \end{aligned} \tag{22}$$

Then, we obtain the associated characteristic equation of model (21) as follows:

$$\begin{aligned} &\lambda^3 + B\lambda^2 + C\lambda + D\lambda e^{-\lambda\tau_1} + Ee^{-\lambda\tau_1} + F\lambda e^{-\lambda\tau_2} \\ &\quad + Ge^{-\lambda\tau_2} = 0, \end{aligned} \tag{23}$$

where

$$\begin{aligned} B &= -(a_{11} + a_{22}); \\ C &= a_{11}a_{22}; \\ D &= -a_{13}a_{31}; \\ E &= a_{13}a_{31}a_{22}; \\ F &= -a_{23}a_{32}; \\ G &= a_{11}a_{23}a_{32}. \end{aligned} \tag{24}$$

Case 1. $\tau_1 > 0, \tau_2 = 0$.

Due to $\tau_1 > 0, \tau_2 = 0$, (23) becomes

$$\lambda^3 + B\lambda^2 + (C+F)\lambda + (D\lambda + E)e^{-\lambda\tau_1} + G = 0. \tag{25}$$

Assuming $\lambda = i\omega_1 (\omega_1 > 0)$ is the pure imaginary root of (25), then the following can be obtained:

$$\begin{aligned} -\omega_1^3 + (C+F)\omega_1 &= E\sin(\omega_1\tau_1) - D\omega_1\cos(\omega_1\tau_1), \\ -B\omega_1^2 + G &= -E\cos(\omega_1\tau_1) - D\omega_1\sin(\omega_1\tau_1), \end{aligned} \tag{26}$$

Then

$$\begin{aligned} &\omega_1^6 + \left(B^2 - 2(C+F)\right)\omega_1^4 \\ &\quad + \left((C+F)^2 - 2BG - D^2\right)\omega_1^2 + G^2 - E^2 = 0. \end{aligned} \tag{27}$$

Now, we define a function as follows:

$$\begin{aligned} f_1(v_1) &= v_1^3 + \left(B^2 - 2(C+F)\right)v_1^2 \\ &\quad + \left((C+F)^2 - 2BG - D^2\right)v_1 + G^2 - E^2. \end{aligned} \tag{28}$$

(i) If (H_{21}):$G^2 - E^2 < 0$ holds, then, (28) has at least one positive root. Without loss of generality, we denote v_{11}, v_{12}, and v_{13} as the roots of (28); hence $\omega_{1k} = \sqrt{v_{1k}}$, $k = 1, 2, 3$, if $v_{1k} > 0$.

(ii) If (H_{22}):$G^2 - E^2 > 0$ holds, let $M_1 = B^2 - 2(C+F)$ and $M_2 = (C+F)^2 - 2BG - D^2$. When $\Delta = {M_1}^2 - 3M_2 \leq 0$, then (28) has no positive roots. However, when $\Delta > 0$, $f_1'(v_1) = 0$ has two real roots, denoted as

$$\begin{aligned} x_1^* &= \frac{-M_1 + \sqrt{\Delta}}{3}, \\ x_2^* &= \frac{-M_1 - \sqrt{\Delta}}{3}. \end{aligned} \tag{29}$$

Obviously, $\lim_{x\longrightarrow+\infty} f_1(x) = +\infty$. If (H_{22}) and $\Delta = {M_1}^2 - 3M_2 > 0$ holds, then (28) has two positive real roots if and only if $x_1^* > 0$ and $f_1(x_1^*) < 0$. In addition, we denote two positive roots of (28) as χ_1 and χ_2; then, (27) has two positive roots, namely, $\omega_{1a} = \sqrt{\chi_1}$ and $\omega_{1b} = \sqrt{\chi_2}$. Furthermore, we can have the following results.

Proposition 7.

(i) *If (H_{21}) holds, then (28) has at least one positive root.*

(ii) *If (H_{22}) and $\Delta = {M_1}^2 - 3M_2 \le 0$ holds, then, (28) has no positive root.*

(iii) *If (H_{22}) and $\Delta = {M_1}^2 - 3M_2 > 0$ holds, then, (28) has two positive roots if and only if $x_1^* > 0$, and $f_1(x_1^*) < 0$.*

Then, according to (26), the critical delay can be obtained as follows:

$$\tau_{1p}^j = \frac{1}{\omega_{1p}} \left(\arccos \frac{D\omega_{1p}^4 + (BE - (CD + DF))\,\omega_{1p}^2 - EG}{D^2\omega_{1p}^2 + E^2} + 2j\pi \right), \quad j = 0, 1, 2, \ldots, \quad p = 1, 2, 3, a, b \tag{30}$$

Letting $\tau_{10} = \min_{p=1,2,3,a,b} \tau_{1p}^0$, from [37] we know that $\operatorname{Re}(d\lambda/d\tau_1) \ne 0$ also needs to be proved. Differentiating left side of (26) with respect to τ_1, we have

$$\left(\frac{d\lambda}{d\tau_1}\right)^{-1} = \frac{3\lambda^2 + 2B\lambda + (C + F) + De^{-\lambda\tau_1}}{\lambda\,(D\lambda + E)\,e^{-\lambda\tau_1}} - \frac{\tau_1}{\lambda}, \tag{31}$$

so that the following can be obtained:

$$\operatorname{Re}\left(\frac{d\lambda}{d\tau_1}\right)^{-1}_{\lambda=i\omega_{10}} = \frac{\omega_{10}^2}{\Delta} {f_1}'\left(\omega_{10}^2\right), \tag{32}$$

where

$$\Delta = \left(-D\omega_{10}^2 \cos\left(\omega_{10}\tau_1\right) + E\omega_{10} \sin\left(\omega_{10}\tau_1\right)\right)^2 + \left(E\omega_{10}\cos\left(\omega_{10}\tau_1\right) + D\omega_{10}^2\sin\left(\omega_{10}\tau_1\right)\right)^2. \tag{33}$$

If (i) in Proposition 7 and (H_{23}): ${f_1}'(\omega_{10}^2) \ne 0$ hold, then we have $\operatorname{Re}(d\lambda/d\tau_1)^{-1}_{\lambda=i\omega_{10}} \ne 0$. However, if (iii) in Proposition 7 holds, assuming $\tau_{1a}^j < \tau_{1b}^j$, then we obtain ${f_1}'(\chi_1) > 0$ and ${f_1}'(\chi_2) < 0$. Hence, we have $(d\operatorname{Re}\lambda(\tau)/d\tau)|_{\tau=\tau_{1a}^j} > 0$, $(d\operatorname{Re}\ \lambda(\tau)/d\tau)|_{\tau=\tau_{1b}^j} < 0$, and $j = 0, 1, 2, \ldots$. Therefore, we have the following results.

Theorem 8. *For model (1) with $\tau_1 > 0$, $\tau_2 = 0$,*

(i) *If (H_{21}) and (H_{23}) both hold, then the positive equilibrium E_* is locally asymptotically stable for $\tau_1 \in (0, \tau_{10})$ and Hopf bifurcation occurs at $\tau_1 = \tau_{10}$.*

(ii) *If (ii) in Proposition 7 holds, then the positive equilibrium E_* is locally asymptotically stable for all $\tau_1 \ge 0$.*

(iii) *If (iii) in Proposition 7 holds, there exists a nonnegative integer n, such that the positive equilibrium E_* is locally asymptotically stable whenever $\tau_1 \in [0, \tau_{1a}^0) \cup (\tau_{1b}^0, \tau_{1a}^1) \cup \cdots \cup (\tau_{1b}^{n-1}, \tau_{1a}^n)$ and is unstable whenever $\tau_1 \in [\tau_{1a}^0, \tau_{1b}^0) \cup (\tau_{1a}^1, \tau_{1b}^1) \cup \cdots \cup (\tau_{1a}^{n-1}, \tau_{1b}^{n-1}) \cup (\tau_{1a}^n, +\infty)$. Then, model (1) undergoes Hopf bifurcation around E_* at every $\tau_1 = \tau_{1a}^j$ and τ_{1b}^j, $j = 0, 1, 2, \ldots$.*

Case 2. $\tau_1 = 0$, $\tau_2 > 0$.

Since $\tau_1 = 0$, $\tau_2 > 0$, (23) becomes

$$\lambda^3 + B\lambda^2 + (C + D)\,\lambda + (F\lambda + G)\,e^{-\lambda\tau_2} + E = 0. \tag{34}$$

Similar to Case 1, let $\lambda = i\omega_2 (\omega_2 > 0)$ be the pure imaginary root of (34); then we obtain

$$\begin{aligned} -\omega_2^3 + (C + D)\,\omega_2 &= G\sin\left(\omega_2\tau_2\right) - F\omega_2\cos\left(\omega_2\tau_2\right), \\ -B\omega_2^2 + E &= G\cos\left(\omega_2\tau_2\right) - F\omega_2\sin\left(\omega_2\tau_2\right). \end{aligned} \tag{35}$$

That is,

$$\omega_2^6 + \left(B^2 - 2\,(C + D)\right)\omega_2^4 + \left((C + D)^2 - 2BE - F^2\right)\omega_2^2 + E^2 - G^2 = 0. \tag{36}$$

Letting $v_2 = \omega_2^2$, we define the following function:

$$f_2\left(v_2\right) = v_2^3 + \left(B^2 - 2\,(C + D)\right)v_2^2 + \left((C + D)^2 - 2BE - F^2\right)v_2 + E^2 - G^2. \tag{37}$$

(i) If (H_{31}):$E^2 - G^2 < 0$ holds, then (37) has at least one positive root. Without loss of generality, we denote v_{21}, v_{22}, v_{23} as the roots of (37); then $\omega_{2k} = \sqrt{v_{2k}}$, $k = 1, 2, 3$, if $v_{2k} > 0$.

(ii) If (H_{32}):$E^2 - G^2 > 0$ holds, let $M_1 = B^2 - 2(C + D)$ and $M_2 = (C + D)^2 - 2BE - F^2$. When $\Delta = {M_1}^2 - 3M_2 \le 0$, then (37) has no positive roots. However, when $\Delta > 0$, $f_2'(v_2) = 0$ has two real roots, denoted as

$$\begin{aligned} x_1^{**} &= \frac{-M_1 + \sqrt{\Delta}}{3}, \\ x_2^{**} &= \frac{-M_1 - \sqrt{\Delta}}{3}. \end{aligned} \tag{38}$$

Obviously, $\lim_{x\longrightarrow+\infty} f_2(x) = +\infty$. If (H_{32}) and $\Delta = {M_1}^2 - 3M_2 > 0$ holds, then (37) has two positive real roots if and only if $x_1^{**} > 0$ and $f_2(x_1^{**}) < 0$. In addition, we denote two positive roots of (37) as χ_1^* and χ_2^*; then (36) has two positive roots, namely, $\omega_{2a} = \sqrt{\chi_1^*}$ and $\omega_{2b} = \sqrt{\chi_2^*}$. Furthermore, we can obtain the following results.

Proposition 9.

(i) *If (H_{31}) holds, then (36) has at least one positive root.*

(ii) *If (H_{32}) and $\Delta = {M_1}^2 - 3M_2 \le 0$ holds, then, (36) has no positive root.*

(iii) *If (H_{32}) and $\Delta = {M_1}^2 - 3M_2 > 0$ holds, then, (36) has two positive roots if and only if $x_1^{**} > 0$ and $f_2(x_1^{**}) < 0$.*

Then the critical delay can be derived by (35):

$$\tau_{2p}^{j} = \frac{1}{\omega_{2p}}\left(\arccos\frac{D\omega_{2p}^{4} + (BE - (CD + DF))\,\omega_{2p}^{2} - EG}{D^{2}\omega_{2p}^{2} + E^{2}} + 2j\pi\right), \quad j = 0, 1, 2, \ldots, \quad p = 1, 2, 3, a, b \tag{39}$$

Let $\tau_{20} = \min_{p=1,2,3,a,b}\tau_{2p}^{0}$. Differentiating left side of (34) with respect to τ_2, we obtain

$$\left(\frac{d\lambda}{d\tau_2}\right)^{-1} = \frac{3\lambda^2 + 2B\lambda + (C + D) + Fe^{-\lambda\tau_2}}{\lambda\,(F\lambda + G)\,e^{-\lambda\tau_2}} - \frac{\tau_2}{\lambda}, \tag{40}$$

Hence, we obtain the following:

$$\operatorname{Re}\left(\frac{d\lambda}{d\tau_2}\right)^{-1}_{\lambda = i\omega_{20}} = \frac{\omega_{20}^{2}}{\Delta} f_2{}'\left(\omega_{20}^{2}\right), \tag{41}$$

where

$$\Delta = \left(-F\omega_{20}^{2}\cos\left(\omega_{20}\tau_2\right) + G\omega_{20}\sin\left(\omega_{20}\tau_2\right)\right)^{2} + \left(G\omega_{20}\cos\left(\omega_{20}\tau_2\right) + F\omega_{20}^{2}\sin\left(\omega_{20}\tau_2\right)\right)^{2}. \tag{42}$$

If (i) in Proposition 9 and (H_{33}): $f_2{}'(\omega_{20}^2) \neq 0$ both hold, then $\operatorname{Re}(d\lambda/d\tau_2)^{-1}_{\lambda=i\omega_{20}} \neq 0$ is obtained. However, if (iii) in Proposition 9 holds, assuming $\tau_{2a}^{j} < \tau_{2b}^{j}$, we obtain $f_2{}'(\chi_1^*) > 0$ and $f_2{}'(\chi_2^*) < 0$. Then, we have $(d\operatorname{Re}\lambda(\tau)/d\tau)|_{\tau=\tau_{2a}^{j}} > 0$, $(d\operatorname{Re}\lambda(\tau)/d\tau)|_{\tau=\tau_{2b}^{j}} < 0$, and $j = 0, 1, 2, \ldots$. Therefore, we have the following theorem.

Theorem 10. *For model (1) with $\tau_1 = 0$, $\tau_2 > 0$,*

(i) *If H_{31} and H_{33} hold, then, the positive equilibrium E_* is locally asymptotically stable for $\tau_2 \in (0, \tau_{20})$ and Hopf bifurcation occur at $\tau_2 = \tau_{20}$.*

(ii) *If (ii) in Proposition 9 holds, then the positive equilibrium E_* is locally asymptotically stable for all $\tau_2 \geq 0$.*

(iii) *If (iii) in Proposition 9 holds, then there exists a non-negative integer n, such that the positive equilibrium E_* is locally asymptotically stable whenever $\tau_2 \in [0, \tau_{2a}^{0}) \cup (\tau_{2b}^{0}, \tau_{2a}^{1}) \cup \cdots \cup (\tau_{2b}^{n-1}, \tau_{2a}^{n})$ and is unstable whenever $\tau_2 \in [\tau_{2a}^{0}, \tau_{2b}^{0}) \cup (\tau_{2a}^{1}, \tau_{2b}^{1}) \cup \cdots \cup (\tau_{2a}^{n-1}, \tau_{2b}^{n-1}) \cup (\tau_{2a}^{n}, +\infty)$. Then, model (1) undergoes Hopf bifurcation around E_* for every $\tau_2 = \tau_{2a}^{j}$ and τ_{2b}^{j}, $j = 0, 1, 2, \ldots$.*

Case 3. $\tau_1 = \tau_2 = \tau$.

When $\tau_1 = \tau_2 = \tau$, (23) becomes

$$\lambda^3 + B\lambda^2 + C\lambda + (D + F)\,\lambda e^{-\lambda\tau} + (E + G)\,e^{-\lambda\tau} = 0. \tag{43}$$

Leting $\lambda = i\omega_3 (\omega_3 > 0)$ be the pure imaginary root of (43), then

$$\begin{aligned} -\omega_3^3 + C\omega_3 &= (E + G)\sin\left(\omega_3\tau\right) - (D + F)\,\omega_3\cos\left(\omega_3\tau\right), \\ -B\omega_3^2 &= -(E + G)\cos\left(\omega_3\tau\right) - (D + F)\,\omega_3\sin\left(\omega_3\tau\right), \end{aligned} \tag{44}$$

that is,

$$\omega_3^6 + \left(B^2 - 2C\right)\omega_3^4 + \left[C^2 - (D + F)^2\right]\omega_3^2 - (E + G)^2 = 0. \tag{45}$$

Let $v_3 = \omega_3^2$ and define the following function:

$$f_3\left(v_3\right) = v_3^3 + \left(B^2 - 2C\right)v_3^2 + \left[C^2 - (D + F)^2\right]v_3 - (E + G)^2, \tag{46}$$

From (46), we can clearly see that $f_3(0) = -(E + G)^2 < 0$; hence (46) has at least one positive root. Without loss of generality, we denote v_{31}, v_{32}, and v_{33} as the roots of (46); then we have $\omega_{3k} = \sqrt{v_{3k}}$, $k = 1, 2, 3$, if $v_{3k} > 0$ holds. Hence, the critical delay can be derived by (44):

$$\tau_{3k}^{j} = \frac{1}{\omega_{3k}}\left(\arccos\frac{(D + F)\,\omega_{3k}^{4} + B\,(E + G)\,\omega_{3k}^{2} - C\,(D + F)\,\omega_{3k}^{2}}{(D + F)^{2}\,\omega_{3k}^{2} + (E + G)^{2}} + 2\pi j\right), \quad (j = 0, 1, 2\ldots, \; k = 1, 2, 3). \tag{47}$$

Let $\tau_{30} = \min_{k=1,2,3}\tau_{3k}^{0}$. Differentiating left side of (43) with respect to τ, we obtain

$$\left(\frac{d\lambda}{d\tau}\right)^{-1} = \frac{3\lambda^2 + 2B\lambda + C + (D + F)\,e^{-\lambda\tau}}{\lambda\left[(D + F)\,\lambda + (E + G)\right]e^{-\lambda\tau}} - \frac{\tau}{\lambda}. \tag{48}$$

Hence, we obtain the following:

$$\operatorname{Re}\left(\frac{d\lambda}{d\tau}\right)^{-1}_{\lambda = i\omega_{30}} = \frac{\omega_{30}^{2}}{\Delta} f_3{}'\left(\omega_{30}^{2}\right), \tag{49}$$

where

$$\Delta = \left(-(D + F)\,\omega_{30}^{2}\cos\left(\omega_{30}\tau\right) + (E + G)\,\omega_{30}\sin\left(\omega_{30}\tau\right)\right)^{2} + \left((E + G)\,\omega_{30}\cos\left(\omega_{30}\tau\right) + (D + F) \cdot \omega_{30}^{2}\sin\left(\omega_{30}\tau\right)\right)^{2}. \tag{50}$$

If (H_{41}): $f_3{}'(\omega_{30}^2) \neq 0$ holds, then $\mathrm{Re}(d\lambda/d\tau)^{-1}_{\lambda=i\omega_{30}} \neq 0$ is obtained; hence, we have the following result.

Theorem 11. *For model (1), when $\tau_1 = \tau_2 = \tau$, if (H_{41}) holds, then the positive equilibrium E_* is locally asymptotically stable for $\tau \in (0, \tau_{30})$ and Hopf bifurcation occurs at $\tau = \tau_{30}$.*

Case 4. $\tau_1 \in (0, \tau_{10})$, $\tau_2 > 0$.

Under this case, τ_2 is considered as a parameter. The same as Case 1, let $\lambda = i\omega_2^*$ be the root of (23); then we have the following:

$$\begin{aligned} R_{51}\cos(\omega_2^*\tau_2) - R_{52}\sin(\omega_2^*\tau_2) &= R_{53}, \\ R_{51}\sin(\omega_2^*\tau_2) + R_{52}\cos(\omega_2^*\tau_2) &= R_{54}, \end{aligned} \tag{51}$$

where

$$\begin{aligned} R_{51} &= F\omega_2^*; \\ R_{53} &= {\omega_2^*}^3 - C\omega_2^* - D\omega_2^*\cos(\omega_2^*\tau_1) + E\sin(\omega_2^*\tau_1); \\ R_{52} &= G; \\ R_{54} &= B{\omega_2^*}^2 - D\omega_2^*\sin(\omega_2^*\tau_1) - E\cos(\omega_2^*\tau_1). \end{aligned} \tag{52}$$

According to (51), the following holds:

$$\begin{aligned} &F_1(\omega_2^*) + F_2(\omega_2^*)\sin(\omega_2^*\tau_1) + F_3(\omega_2^*)\cos(\omega_2^*\tau_1) \\ &\quad = 0, \end{aligned} \tag{53}$$

where

$$\begin{aligned} F_1(\omega_2^*) &= {\omega_2^*}^6 + (B^2 - 2C){\omega_2^*}^4 \\ &\quad + (C^2 + D^2 - F^2){\omega_2^*}^2 + (E^2 - G^2), \\ F_2(\omega_2^*) &= 2(E - BD){\omega_2^*}^3 - 2CE\omega_2^*, \\ F_3(\omega_2^*) &= -2D{\omega_2^*}^4 + 2(CD - BE){\omega_2^*}^2. \end{aligned} \tag{54}$$

Assuming (H_{51}): (53) has finite positive root and denoting as ω_{2k}^*, $(k = 1, 2, \ldots, l_1)$, then the critical value can be represented as follows:

$$\begin{aligned} &{\tau_{2k}^*}^{(j)} \\ &= \frac{1}{\omega_{2k}^*}\left(\arccos\left(\frac{R_{51}\cdot R_{53} + R_{52}\cdot R_{54}}{R_{51}^2 + R_{52}^2}\right) + 2\pi j\right), \\ &\qquad (j = 0, 1, 2\ldots;\ k = 1, 2, \ldots l_1). \end{aligned} \tag{55}$$

Let $\tau_{20}^* = \min {\tau_{2k}^*}^{(0)}$, $(k = 1, 2, \ldots l_1)$. Differentiating left side of (23) with respect to τ_2, the following is obtained:

$$\begin{aligned} &\left(\frac{d\lambda}{d\tau_2}\right)^{-1} \\ &= \frac{3\lambda^2 + 2B\lambda + C + (D - D\lambda\tau_1 - \tau_1 E)e^{-\lambda\tau_1} + Fe^{-\lambda\tau_2}}{\lambda(F\lambda + G)e^{-\lambda\tau_2}} \\ &\quad - \frac{\tau_2}{\lambda}, \end{aligned} \tag{56}$$

and then, we have

$$\mathrm{Re}\left(\frac{d\lambda}{d\tau_2}\right)^{-1}_{\lambda=i\omega_{20}^*} = \frac{F_{51}F_{53} + F_{54}F_{52}}{F_{51}^2 + F_{52}^2}, \tag{57}$$

where

$$\begin{aligned} F_{51} &= -F{\omega_{20}^*}^2\cos(\omega_{20}^*\tau_{20}^*) + G\omega_{20}^*\sin(\omega_{20}^*\tau_{20}^*), \\ F_{52} &= G\omega_{20}^*\cos(\omega_{20}^*\tau_{20}^*) + F{\omega_{20}^*}^2\sin(\omega_{20}^*\tau_{20}^*), \\ F_{53} &= -3{\omega_{20}^*}^2 + C + D\cos(\omega_{20}^*\tau_1) - \tau_1 E\cos(\omega_{20}^*\tau_1) \\ &\quad - \tau_1 D\omega_{20}^*\sin(\omega_{20}^*\tau_1) + F\cos(\omega_{20}^*\tau_{20}^*), \\ F_{54} &= 2B\omega_{20}^* - D\sin(\omega_{20}^*\tau_1) + \tau_1 E\sin(\omega_{20}^*\tau_1) \\ &\quad - \tau_1 D\omega_{20}^*\cos(\omega_{20}^*\tau_1) - F\sin(\omega_{20}^*\tau_{20}^*). \end{aligned} \tag{58}$$

Supposing (H_{52}): $F_{51}F_{53} + F_{54}F_{52} \neq 0$, then we have the following.

Theorem 12. *For model (1), when $\tau_1 \in (0, \tau_{10})$ and $\tau_2 > 0$, if both H_{51} and H_{52} hold, then the positive equilibrium E_* is locally asymptotically stable for $\tau_2 \in (0, \tau_{20}^*)$ and Hopf bifurcation occurs at $\tau_2 = \tau_{20}^*$.*

Case 5. $\tau_1 > 0$, $\tau_2 \in (0, \tau_{20})$.

Since $\tau_1 > 0$, $\tau_2 \in (0, \tau_{20})$, we consider τ_1 as a parameter. The same as Case 4, letting $\lambda = i\omega_1^*$ be the root of (23), we obtain:

$$\begin{aligned} R_{61}\cos(\omega_1^*\tau_1) - R_{62}\sin(\omega_1^*\tau_1) &= R_{63}, \\ R_{61}\sin(\omega_1^*\tau_1) + R_{62}\cos(\omega_1^*\tau_1) &= R_{64}, \end{aligned} \tag{59}$$

where

$$\begin{aligned} R_{61} &= D\omega_1^*; \\ R_{63} &= {\omega_1^*}^3 - C\omega_1^* - F\omega_1^*\cos(\omega_1^*\tau_2) + G\sin(\omega_1^*\tau_2); \\ R_{62} &= E; \\ R_{64} &= B{\omega_1^*}^2 - F\omega_1^*\sin(\omega_1^*\tau_2) - G\cos(\omega_1^*\tau_2). \end{aligned} \tag{60}$$

According to (59), the following holds:

$$\begin{aligned} &G_1(\omega_1^*) + G_2(\omega_1^*)\sin(\omega_1^*\tau_2) + G_3(\omega_1^*)\cos(\omega_1^*\tau_2) \\ &\quad = 0, \end{aligned} \tag{61}$$

where

$$\begin{aligned} G_1(\omega_1^*) &= {\omega_1^*}^6 + (B^2 - 2C){\omega_1^*}^4 \\ &\quad + (C^2 + F^2 - D^2){\omega_1^*}^2 + (G^2 - E^2), \\ G_2(\omega_1^*) &= 2(G - BF){\omega_1^*}^3 - 2CG\omega_1^*, \\ G_3(\omega_1^*) &= -2F{\omega_1^*}^4 + 2(CF - BG){\omega_2^*}^2. \end{aligned} \tag{62}$$

Supposing (H_{61}): (61) has finite positive root ω_{2k}^*, $(k = 1, 2, \ldots, l_2)$, then we obtain

$$\tau_{1k}^{*\,(j)} = \frac{1}{\omega_{1k}^*}\left(\arccos\left(\frac{R_{61}\cdot R_{63} + R_{62}\cdot R_{64}}{R_{61}^2 + R_{62}^2}\right) + 2\pi j\right), \quad (j = 0, 1, 2\ldots;\ k = 1, 2, \ldots l_2). \tag{63}$$

Assuming $\tau_{10}^* = \min \tau_{1k}^{*\,(0)}$, $(k = 1, 2, \ldots l_2)$ and differentiating left side of (23) with respect to τ_1, therefore, the following is obtained:

$$\left(\frac{d\lambda}{d\tau_1}\right)^{-1} = \frac{3\lambda^2 + 2B\lambda + C + (F - F\lambda\tau_2 - \tau_2 G)e^{-\lambda\tau_2} + De^{-\lambda\tau_1}}{\lambda(F\lambda + G)e^{-\lambda\tau_2}} - \frac{\tau_1}{\lambda}, \tag{64}$$

Hence, we have

$$\operatorname{Re}\left(\frac{d\lambda}{d\tau_1}\right)^{-1}_{\lambda = i\omega_{10}^*} = \frac{F_{61}F_{63} + F_{64}F_{62}}{F_{61}^2 + F_{62}^2}, \tag{65}$$

where

$$\begin{aligned}
F_{61} &= -D\omega_{10}^{*\,2}\cos(\omega_{10}^*\tau_{10}^*) + E\omega_{10}^*\sin(\omega_{10}^*\tau_{10}^*),\\
F_{62} &= E\omega_{10}^*\cos(\omega_{10}^*\tau_{10}^*) + D\omega_{10}^{*\,2}\sin(\omega_{10}^*\tau_{10}^*),\\
F_{63} &= -3\omega_{10}^{*\,2} + C + D\cos(\omega_{10}^*\tau_{10}^*) - \tau_2 G\cos(\omega_{10}^*\tau_2)\\
&\quad - \tau_2 F\omega_{10}^*\sin(\omega_{10}^*\tau_2) + F\cos(\omega_{10}^*\tau_2),\\
F_{64} &= 2B\omega_{10}^* - D\sin(\omega_{10}^*\tau_{10}^*) + \tau_2 G\sin(\omega_{10}^*\tau_2)\\
&\quad - \tau_2 F\omega_{10}^*\cos(\omega_{10}^*\tau_2) - F\sin(\omega_{10}^*\tau_2),
\end{aligned} \tag{66}$$

Supposing (H_{62}): $F_{61}F_{63} + F_{64}F_{62} \neq 0$ holds, then we obtain the following theorem.

Theorem 13. *For model (1), when $\tau_1 > 0$ and $\tau_2 \in (0, \tau_{20})$, if both H_{61} and H_{62} hold, then the positive equilibrium E_* is locally asymptotically stable for $\tau_1 \in (0, \tau_{10}^*)$ and Hopf bifurcation occurs at $\tau_1 = \tau_{10}^*$.*

4. Properties of Periodic Solution

In this section, we will discuss the direction of Hopf bifurcation and the stability of the bifurcating periodic solutions under Case 4 by using normal form method and center manifold theorem [43], and methods of other four cases are similar to Case 4. Assuming $\tau_1 \in (0, \tau_{10})$, $\tau_{20}^* > \tau_1$, and Hopf bifurcation occurs at (N^*, P^*, A^*) in model (1) when $\tau = \tau_{20}^*$.

Let $\tau_2 = \tau_{20}^* + \mu$, $t = s\tau_2$, $x(s\tau_2) = \widehat{x}(s)$, $y(s\tau_2) = \widehat{y}(s)$, and $z = (s\tau_2) = \widehat{z}(s)$, and we also denote $\widehat{x}(s)$, $\widehat{y}(s)$, and $\widehat{z}(s)$ as $x(s)$, $y(s)$, and $z(s)$. Then, model (1) could be rewritten as follows in $C = C([-1, 0], R^3)$:

$$\dot{u}(t) = L_\mu(u_t) + f(\mu, u_t), \tag{67}$$

where $u(t) = (x(t), y(t), z(t))^T \in R^3$. $L_\mu(\phi) : C \longrightarrow R^3$ and $f(\mu, u(t))$ are given as follows:

$$\begin{aligned}
L_\mu(\phi) &= (\tau_{20}^* + \mu)\left(A\phi(0) + B\phi\left(-\frac{\tau_1}{\tau_{20}^*}\right) + C\phi(-1)\right),\\
f(\mu, \phi) &= (\tau_{20}^* + \mu)\begin{pmatrix} f_1 & f_2 & f_3\end{pmatrix}^T,
\end{aligned} \tag{68}$$

where

$$\begin{aligned}
A &= \begin{pmatrix} a_{11} & 0 & a_{13}\\ 0 & a_{22} & a_{23}\\ 0 & 0 & 0\end{pmatrix},\\
B &= \begin{pmatrix} 0 & 0 & 0\\ 0 & 0 & 0\\ a_{31} & 0 & 0\end{pmatrix},\\
C &= \begin{pmatrix} 0 & 0 & 0\\ 0 & 0 & 0\\ 0 & a_{32} & 0\end{pmatrix},\\
f_1 &= -\alpha_1\phi_1(0)\phi_3(0),\\
f_2 &= -\alpha_2\phi_2(0)\phi_3(0),\\
f_3 &= \beta_1\alpha_1\phi_1\left(-\frac{\tau_1}{\tau_{20}^*}\right)\phi_3(0) + \beta_2\alpha_2\phi_2(-1)\phi_3(0).
\end{aligned} \tag{69}$$

According to the Riesz representation theorem, we know that there exists a function $\eta(\theta, \mu)$ of bounded variation for $\theta \in [-1, 0]$ such that $L_\mu\phi = \int_{-1}^{0} d\eta(\theta, \mu)\phi(\theta)$, for all $\phi \in C([-1, 0], R^3)$. Choosing

$$\eta(\theta, \mu) = \begin{cases} (\tau_{20}^* + \mu)(A + B + C), & \theta = 0\\ (\tau_{20}^* + \mu)(B + C), & \theta \in \left[-\dfrac{\tau_1}{\tau_{20}^*}, 0\right)\\ (\tau_{20}^* + \mu)C, & \theta \in \left(-1, -\dfrac{\tau_1}{\tau_{20}^*}\right)\\ 0, & \theta = -1 \end{cases} \tag{70}$$

For $\phi \in C^1([-1,\ 0], R^3)$, we define

$$A(\mu)\phi = \begin{cases} \dfrac{d\phi(\theta)}{d\theta}, & \theta \in [-1,0) \\ \displaystyle\int_{-1}^{0} d\eta(\mu,s)\cdot\phi(s), & \theta = 0 \end{cases}$$
$$R(\mu)\phi = \begin{cases} 0, & \theta \in [-1,0) \\ f(\mu,\phi), & \theta = 0 \end{cases} \tag{71}$$

Then, model (1) can be rewritten as

$$\dot{u}(t) = A(\mu)u_t + R(\mu)u_t. \tag{72}$$

For $\psi \in C^1([0,1],(R^3)^*)$, the adjoint operator A^* of A is defined as follows:

$$A^*\psi(s) = \begin{cases} -\dfrac{d\psi(s)}{ds}, & s \in (0,1], \\ \displaystyle\int_{-1}^{0} d\eta^T(t,0)\psi(-t), & s = 0. \end{cases} \tag{73}$$

Associated with a bilinear inner product

$$\langle\psi(s),\phi(\theta)\rangle = \overline{\psi}(0)\phi(0) - \int_{-1}^{0}\int_{\xi=0}^{\theta}\overline{\psi}(\xi-\theta)\,d\eta(\theta)\,\phi(\xi)\,d\xi, \tag{74}$$

where $\eta(\theta) = \eta(\theta,0)$ and we know that $\pm i\omega_{20}^*\tau_{20}^*$ are the eigenvalues of $A(0)$ and $A^*(0)$.

Choose $q(\theta) = (1,q_2,q_3)^T e^{i\omega_{20}^*\tau_{20}^*\theta}$ to be the eigenvector of $A(0)$ corresponding to the eigenvalue $i\omega_{20}^*\tau_{20}^*$ and $q^*(s) = D(1,q_2^*,q_3^*)e^{i\omega_{20}^*\tau_{20}^* s}$ to be the eigenvector of $A^*(0)$ corresponding to the eigenvalue $-i\omega_{20}^*\tau_{20}^*$. By computation, we obtain

$$\begin{aligned} q_2 &= \frac{a_{23}(i\omega_{20}^* - a_{11})}{a_{13}(i\omega_{20}^* - a_{22})}; \\ q_3 &= \frac{i\omega_{20}^* - a_{11}}{a_{13}}; \\ q_2^* &= \frac{a_{32}e^{i\omega_{20}^*\tau_1}(a_{11} + i\omega_2^*)}{a_{31}e^{i\omega_{20}^*\tau_1}(a_{22} + i\omega_2^*)}; \\ q_3^* &= \frac{-(a_{11} + i\omega_2^*)}{a_{31}e^{i\omega_{20}^*\tau_1}}. \end{aligned} \tag{75}$$

Besides, from (74) we have

$$\overline{D} = \frac{1}{1 + q_2\overline{q}_2^* + q_3\overline{q}_3^* + \overline{q}_3^* a_{31}\tau_1 e^{-i\omega_{20}^*\tau_1} + q_2\overline{q}_3^* a_{32}\tau_{20}^* e^{-i\omega_{20}^*\tau_{20}^*}}, \tag{76}$$

such that $\langle q^*(s), q(\theta)\rangle = 1$ and $\langle q^*(s), \overline{q}(\theta)\rangle = 0$.

Then, according to [44], we obtain the following relevant parameter, which helps to determine the direction and stability of Hopf bifurcation:

$$\begin{aligned} g_{20} &= 2\overline{D}\tau_{20}^*\Big(-\alpha_1 q_3 - \alpha_2\overline{q}_2^* q_2 q_3 + \beta_1\alpha_1 q_3\overline{q}_3^* e^{-i\omega_{20}^*\tau_1} \\ &\quad + \beta_2\alpha_2 q_2 q_3\overline{q}_3^* e^{-i\omega_{20}^*\tau_{20}^*}\Big), \\ g_{11} &= \overline{D}\tau_{20}^*\Big[-\alpha_1(q_3 + \overline{q}_3) - \alpha_2\overline{q}_2^*(q_2\overline{q}_3 + \overline{q}_2 q_3) \\ &\quad + \beta_1\alpha_1\overline{q}_3^*\Big(\overline{q}_3 e^{-i\omega_{20}^*\tau_1} + q_3 e^{i\omega_{20}^*\tau_1}\Big) \\ &\quad + \beta_2\alpha_2\overline{q}_3^*\Big(q_2\overline{q}_3 e^{-i\omega_{20}^*\tau_{20}^*} + q_3\overline{q}_2 e^{i\omega_{20}^*\tau_{20}^*}\Big)\Big], \\ g_{02} &= 2\overline{D}\tau_{20}^*\Big(-\alpha_1\overline{q}_3 - \alpha_2\overline{q}_2^*\overline{q}_2\overline{q}_3 + \beta_1\alpha_1\overline{q}_3\overline{q}_3^* e^{i\omega_{20}^*\tau_1} \\ &\quad + \beta_2\alpha_2\overline{q}_2\overline{q}_3\overline{q}_3^* e^{i\omega_{20}^*\tau_{20}^*}\Big), \\ g_{21} &= 2\overline{D}\tau_{20}^*\Big\{-\alpha_1\Big[W_{11}^{(3)}(0) + \frac{1}{2}W_{20}^{(3)}(0) \\ &\quad + \frac{1}{2}\overline{q}_3 W_{20}^{(1)}(0) + q_3 W_{11}^{(1)}(0)\Big] - \alpha_2\overline{q}_2^*\Big[q_2 W_{11}^{(3)}(0) \\ &\quad + \overline{q}_2\frac{1}{2}W_{20}^{(3)}(0) + \frac{1}{2}\overline{q}_3 W_{20}^{(2)}(0) + q_3 W_{11}^{(2)}(0)\Big] \\ &\quad + \overline{q}_3^*\beta_1\alpha_1\Big[q_3 W_{11}^{(1)}\Big(-\frac{\tau_1}{\tau_{20}^*}\Big) + \overline{q}_3\frac{1}{2}W_{20}^{(1)}\Big(-\frac{\tau_1}{\tau_{20}^*}\Big) \\ &\quad + \frac{1}{2}W_{20}^{(3)}(0)e^{i\omega_{20}^*\tau_1} + W_{11}^{(3)}(0)e^{-i\omega_{20}^*\tau_1}\Big] \\ &\quad + \overline{q}_3^*\beta_2\alpha_2\Big[q_3 W_{11}^{(2)}(-1) + \overline{q}_3\frac{1}{2}W_{20}^{(2)}(-1) \\ &\quad + \overline{q}_2\frac{1}{2}W_{20}^{(3)}(0)e^{i\omega_{20}^*\tau_{20}^*} + q_2 W_{11}^{(3)}(0)e^{-i\omega_{20}^*\tau_{20}^*}\Big]\Big\}, \end{aligned} \tag{77}$$

and

$$\begin{aligned} W_{20}(\theta) &= \frac{ig_{20}q(0)}{\omega_{20}^*\tau_{20}^*}e^{i\theta\omega_{20}^*\tau_{20}^*} + \frac{\overline{g}_{02}i}{3\omega_{20}^*\tau_{20}^*}\overline{q}(0)e^{-i\theta\omega_{20}^*\tau_{20}^*} \\ &\quad + E_1 e^{2i\theta\omega_{20}^*\tau_{20}^*}, \\ W_{11}(\theta) &= \frac{-ig_{11}q(0)}{\omega_{20}^*\tau_{20}^*}e^{i\theta\omega_{20}^*\tau_{20}^*} + \frac{\overline{g}_{11}i}{\omega_{20}^*\tau_{20}^*}\overline{q}(0)e^{-i\theta\omega_{20}^*\tau_{20}^*} \\ &\quad + E_2, \end{aligned} \tag{78}$$

where E_1 and E_2 can be determined by the following, respectively:

$$\begin{pmatrix} 2i\omega_{20}^* - a_{11} & 0 & -a_{13} \\ 0 & 2i\omega_{20}^* - a_{22} & -a_{23} \\ -a_{31}e^{-2i\omega_{20}^*\tau_1} & -a_{32}e^{-2i\omega_{20}^*\tau_{20}^*} & 2i\omega_{20}^* \end{pmatrix}\cdot E_1$$

$$= 2\begin{pmatrix} K_{11} \\ K_{21} \\ K_{31} \end{pmatrix},$$

$$\begin{pmatrix} a_{11} & 0 & a_{13} \\ 0 & a_{22} & a_{23} \\ a_{31} & a_{32} & 0 \end{pmatrix} \cdot E_2 = -\begin{pmatrix} K_{12} \\ K_{22} \\ K_{32} \end{pmatrix}, \tag{79}$$

where

$$\begin{aligned} K_{11} &= -\alpha_1 q_3; \\ K_{21} &= -\alpha_2 q_2 q_3; \\ K_{31} &= \beta_1 \alpha_1 q_3 e^{-i\omega_{20}^* \tau_1} + \beta_2 \alpha_2 q_2 q_3 e^{-i\omega_{20}^* \tau_{20}^*}; \\ K_{12} &= -\alpha_1 \left(q_3 + \overline{q}_3\right); \\ K_{22} &= -\alpha_2 \left(q_2 \overline{q}_3 + \overline{q}_2 q_3\right); \\ K_{32} &= \beta_1 \alpha_1 \left(q_3 e^{i\omega_{20}^* \tau_1} + \overline{q}_3 e^{-i\omega_{20}^* \tau_1}\right) \\ &\quad + \beta_2 \alpha_2 \left(\overline{q}_2 q_3 e^{i\omega_{20}^* \tau_{20}^*} + q_2 \overline{q}_3 e^{-i\omega_{20}^* \tau_{20}^*}\right). \end{aligned} \tag{80}$$

Then, we can compute the following values:

$$\begin{aligned} c_1(0) &= \frac{i}{2\omega_{20}^* \tau_{20}^*} \left(g_{20} g_{11} - 2\left|g_{11}\right|^2 - \frac{\left|g_{02}\right|^2}{3} \right) + \frac{g_{21}}{2}, \\ \mu &= -\frac{\operatorname{Re}\left(c_1(0)\right)}{\operatorname{Re} \lambda'\left(\tau_{20}^*\right)}, \\ \beta &= 2 \operatorname{Re}\left(c_1(0)\right), \\ T &= -\frac{\operatorname{Im}\left\{c_1(0)\right\} + \mu_2 \operatorname{Im}\left\{\lambda'\left(\tau_{20}^*\right)\right\}}{\omega_{20}^* \tau_{20}^*}. \end{aligned} \tag{81}$$

This determine the properties of bifurcating periodic solutions and the Hopf bifurcation at $\tau = \tau_{20}^*$. That is,

(i) μ determines the direction of the Hopf bifurcation. Specifically, when $\mu > 0 (< 0)$, the Hopf bifurcation is supercritical (subcritical).

(ii) β determines the stability of the bifurcating periodic solutions; when $\beta < 0 (> 0)$, the bifurcating periodic solution is stable (unstable).

(iii) T determines the period of the bifurcating periodic solutions; when $T > 0 (< 0)$, the period of bifurcating periodic solution increases (decrease).

5. Numerical Simulations

Due to the complexity of model (1), we perform some numerical simulations in this section to investigate further how the delay influences dynamics in model (1). The following parameter values are used $I_1 = I_2 = 0.5$, $q_1 = q_2 = 0.001$, $\alpha_1 = \alpha_2 = 0.08$, $\beta_1 = 0.3$, and $m = 0.8$. Other parameters are chosen as control parameters.

According to the standard linear analysis, when τ_2 is equal to zero, the analysis reveals that the $\beta_2 - \tau_1$ parameter plane is divided into four parts (see Figure 1(a)). In Figure 1(a), before β_2 reaching black dashed line, there exists τ_{10} in model (1) such that the unique positive equilibrium loses its stability when the condition, $\tau_1 > \tau_{10}$, holds. When the locus of β_2 is between black dashed line and green dashed line, the stability switches for positive equilibrium do not exist although (28) has two positive roots, which means that there exists τ_{10} in model (1) such that the unique positive equilibrium loses its stability when the condition, $\tau_1 > \tau_{10}$, holds. However, the stability switches for positive equilibrium emerge when β_2 is beyond green dashed line but it does not reach blue zone. When the locus of β_2 is in blue zone, the unique positive equilibrium is always stable, which suggests that τ_1 cannot influence the stability of the positive equilibrium. When τ_1 equals zero, the similar results for $\beta_2 - \tau_2$ parameter plane are shown in Figure 1(b), but the sequence is reversed. Additionally, according to results in Section 4, we calculate the values of μ, β, and T at $\tau_1 = \tau_{10}$ with $\beta_2 \in (0, 0.3)$, and the corresponding results are shown in Figure 1(c), where we can find that the Hopf bifurcation is supercritical and the bifurcating periodic solutions are stable; especially, the period of the bifurcating periodic solutions increases as β_2 increases. For other cases of τ_1 and τ_2, the same procedures with respect to calculations of μ, β, and T can be performed like Figure 1(c).

As examples corresponding to stability of the positive equilibrium with $\beta_2 = 0.2$, taken $\tau_1 = 1$ and $\tau_1 = 3$ in Figure 1(a), respectively, the corresponding numerical solutions are shown in Figure 2. Obviously, the positive equilibrium is stable because $\tau_1 = 1$ is below τ_{10} (see Figure 2(a)). In contrast, due to $3 = \tau_1$ beyond τ_{10}, a periodic solution exists (see Figure 2(b)). Furthermore, set $\beta_2 = 0.7$, then we have $\tau_{1a}^0 \approx 4.9050 < \tau_{1b}^0 \approx 19.0615 < \tau_{1a}^1 \approx 38.6683$. Taken $\tau_1 = 4$, $\tau_1 = 18$ and $\tau_1 = 21$ in Figure 1(a), respectively, the corresponding numerical solutions are shown in Figure 3. Obviously, the positive equilibrium is stable when $\tau_1 = 4$ and $\tau_1 = 21$ (see Figures 3(a) and 3(c)), but the positive equilibrium is unstable when $\tau_1 = 18$ (see Figure 3(b)), which means that the positive equilibrium can gain its stability again for $\tau_1 > \tau_{10}$. In Figure 3, the same initial values are applied, and other parameter values except for τ_1 are also identical. Clearly, the delay is the principal factor giving rise to the difference among (a), (b), and (c).

Numerical solutions in Figure 3 suggest that the stability switches induced by delay may exist. Hence, the bifurcation diagram in $\tau_1 - \tau_2$ parameter plane is given (see Figure 4(a)). For case $\tau_2 = 0$, there exists a τ_1^* such that the positive equilibrium with respect to $\tau_1 \in (0, \tau_1^*)$ is stable. For case $\tau_1 = 0$, there exists a τ_2^* such that the positive equilibrium with respect to $\tau_2 \in (0, \tau_2^*)$ is stable. Additionally, when $\tau_2 \in (0, \tau_2^*)$, Figure 4(a) shows that τ_{10} exists such that the positive equilibrium with respect to $\tau_1 \in (0, \tau_{10})$ is stable. Likewise, when $\tau_1 \in (0, \tau_1^*)$, Figure 4(a) also display that τ_{20} exists such that the positive equilibrium with respect to $\tau_2 \in$

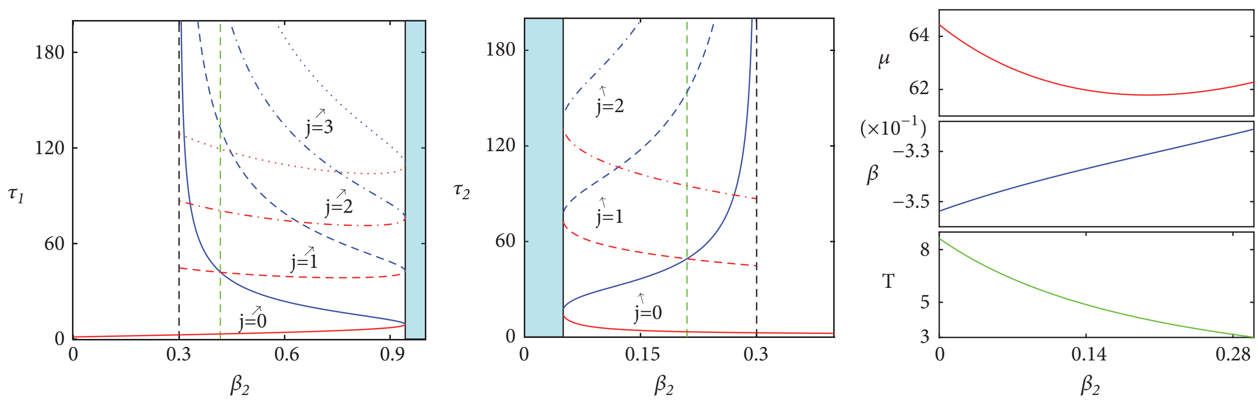

(a) (b) (c)

FIGURE 1: (a) Bifurcation diagram with $\tau_2 = 0$ corresponding to τ_1 V.S. β_2, where solid, dashed, dash-dot, and dotted curves represent the critical values of τ_1 in (30) for j = 0, 1, 2, 3, respectively, and the green dashed line denotes $\beta_2 = 0.417238$. (b) Bifurcation diagram with $\tau_1 = 0$ corresponding to τ_2 V.S. β_2, where solid, dashed, dash-dot, and dotted curves represent the critical values of τ_2 in (39) for j = 0, 1, 2, 3, respectively, and the green dashed line denotes $\beta_2 = 0.21$. (c) Examples for μ, β, and T at $\tau_1 = \tau_{10}$ with respect to β_2, where $\tau_2 = 0$.

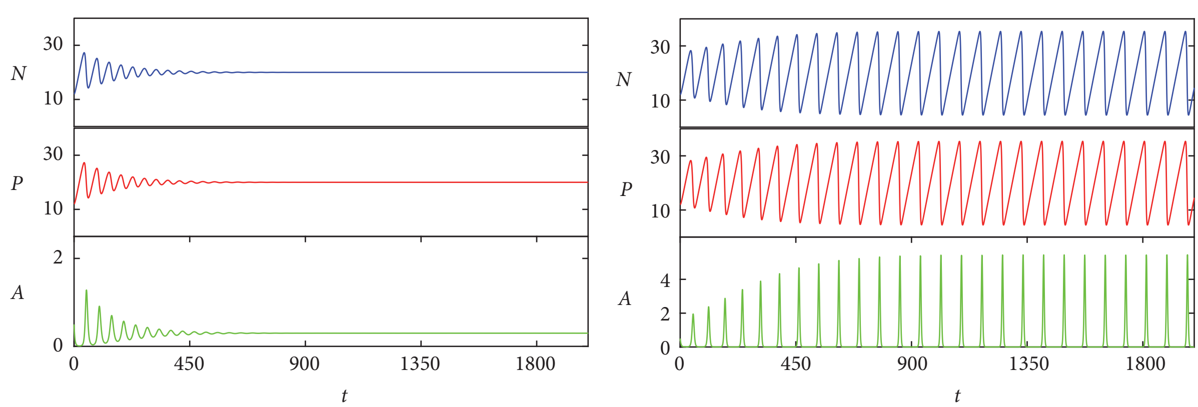

(a) (b)

FIGURE 2: Numerical solutions of model (1) with $\tau_2 = 0$ and $\beta_2 = 0.2$, (a) $\tau_1 = 1$; (b) $\tau_1 = 3$.

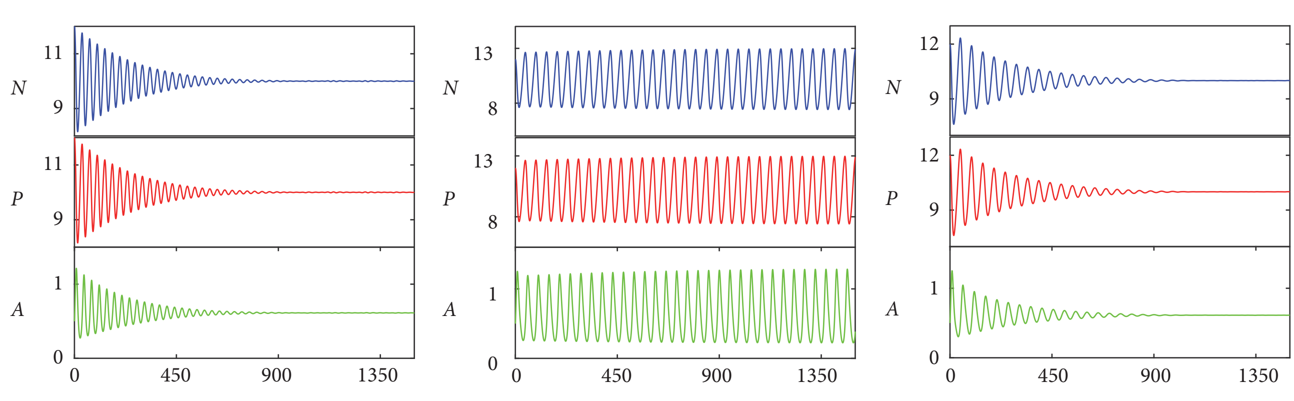

(a) (b) (c)

FIGURE 3: Numerical solutions of model (1) with $\tau_2 = 0$ and $\beta_2 = 0.7$, (a) $\tau_1 = 4$; (b) $\tau_1 = 18$ (c) $\tau_1 = 21$.

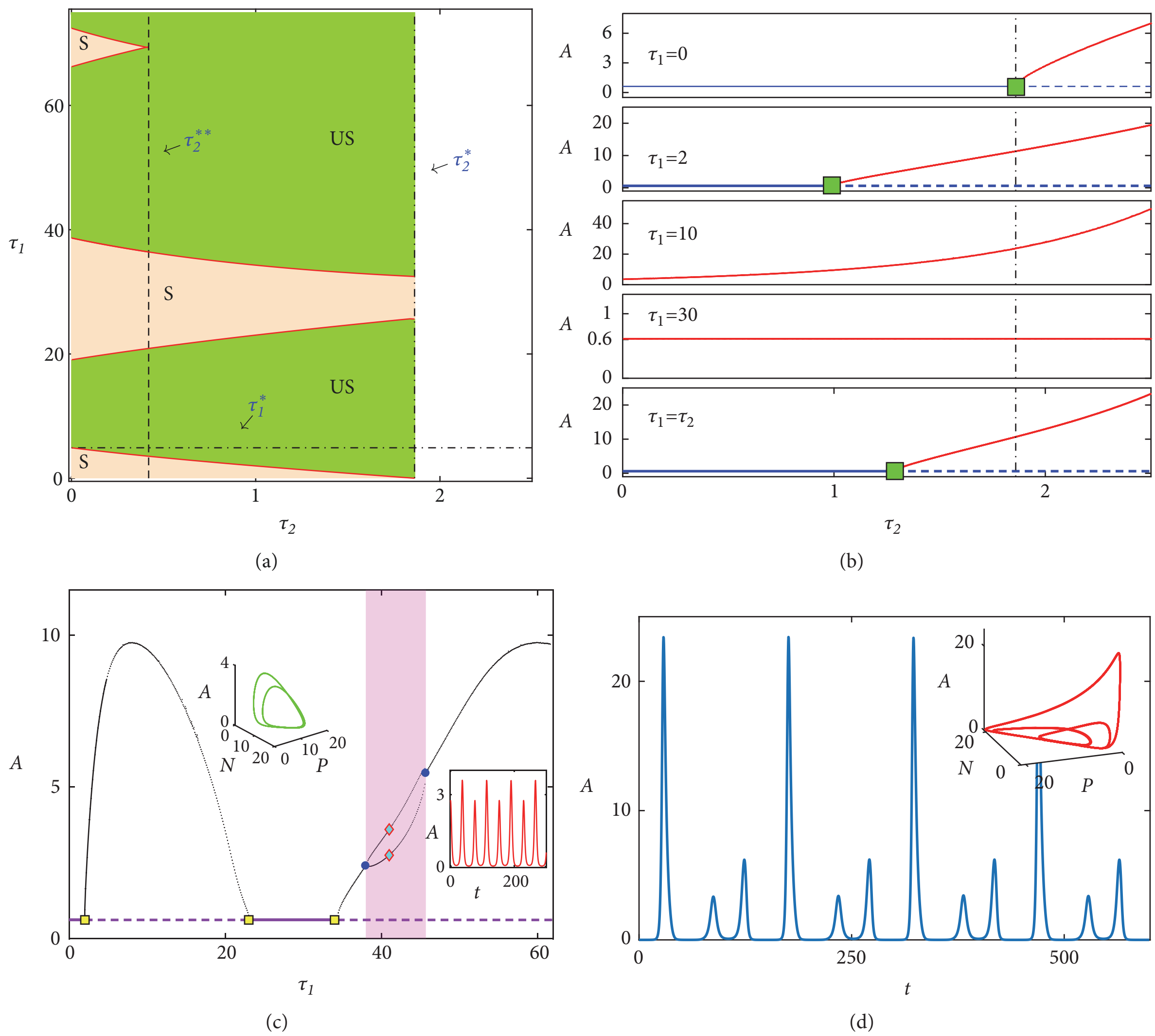

FIGURE 4: (a) Bifurcation diagram with $\beta_2 = 0.7$ for τ_1 V.S. τ_2, where the symbol "S" denotes stable and the symbol "US" denotes unstable; (b) bifurcation diagram with $\beta_2 = 0.7$ for the effect of τ_2 on nutrient-phytoplankton dynamics, where dashed line denotes unstable; solid line denotes stable; the green solid square is Hopf bifurcation point, dot-dashed line corresponding to τ_2^* in (a), blue line represents equilibrium, and red line represents amplitude of periodic solutions. (c) Bifurcation diagram with $\beta_2 = 0.7$ and $\tau_2 = 1$, where the yellow solid square is Hopf bifurcation point, the blue solid circle is bifurcation point for periodic-2 solution, the magenta zone indicates the existence of periodic-2 solutions, and the cyan solid diamond denotes the value of τ_1 for a phase and a time-series in the inner of (c). (d) A periodic-3 solution for phytoplankton population, where $\beta_2 = 0.7$, $\tau_1 = 100$, and $\tau_2 = 2$.

$(0, \tau_{20})$ is stable. Significantly, Figure 4(a) demonstrates that the stability switches for positive equilibrium with respect to τ_1 emerge when τ_2 below τ_2^* is fixed.

Figure 4(b) depicts the dependence of stability of positive equilibrium on delay τ_2 in the fully nonlinear regime for τ_1 in sequence $[0, 2, 10, 30]$ and $\tau_1 = \tau_2$, which is consistent with results in Figure 4(a). However, when τ_2 is fixed, Figure 4(c) shows that the stability switches emerge with τ_1 increases. Especially, periodic-2 solutions exist for some values of τ_2 (see magenta zone in Figure 4(c)). As an example of periodic-2 solution existence, taking $\tau_1 = 41$, a phase and a time-series are given in the inner of Figure 4(c). Moreover, Figure 4(d) shows that there exist periodic-3 solutions in model (1). According to results in Section 2, the positive equilibrium is globally asymptotically stable in the model (1) without delay if it exists. Obviously, the results shown in Figure 4 are induced by delay.

In Figure 4(a), we can find that the number of intervals corresponding to stability of positive equilibrium for small values of τ_2 equals 3. However, when τ_2 is beyond dashed line (τ_2^{**}), the number of intervals is 2. So the number of intervals for stability switches may be different for diverse τ_2. Accordingly, we calculate the number of intervals with respect to parameter β_2, as shown in Figure 5(a). Figure 5(b) shows that there exist 3 stable intervals when $\beta_2 = 0.7$ and $\tau_2 = 0$, which is an example of Figure 5(a). Evidently, parameter β_2 can remarkably influence the number of intervals for stability of positive equilibrium.

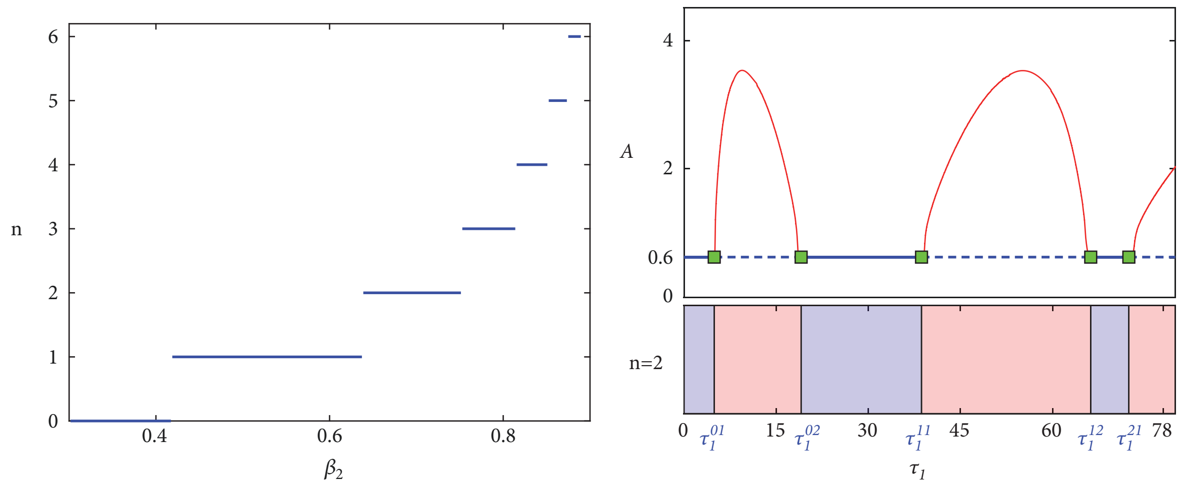

(a) (b)

Figure 5: (a) The number of intervals for stability switches of positive equilibrium with respect to β_2, where $\tau_2 = 0$; (b) based on (a), an example for comparison between results predicted by linear analysis and numerical results in the fully nonlinear regime with (β_2, τ_2) at $(0, 0.7)$, where top panel represents numerical results for model (1) in the fully nonlinear regime; bottom panel depicts the results predicted by linear analysis, and blue and red area denote stable and unstable, respectively.

6. Conclusions

In this paper we proposed a nitrogen-phosphorus-phytoplankton model with multiple delays. The analysis focused on the effect of delay on nutrient-phytoplankton dynamics. In the absence of delay, theoretical analysis indicated that the unique positive equilibrium is globally asymptotically stable in model (1) if it exists. Deng et al. [48] also studied a nitrogen-phosphorus-phytoplankton model without delay, where Holling II function was employed to describe the nutrient uptake dynamics of phytoplankton. Although the function modelling the nutrient uptake dynamics of phytoplankton is different, they get the same results. These results mean that the nutrient-phytoplankton ecosystem will approach the stable equilibrium. However, it has been reported [18] that a constant population density may not exist because of the existence of some factors including noise, interval factors, and physical factors. And ecological studies [49, 50] also criticized this idea of "the balance of nature." Actually, the existence of nutrient-plankton oscillations has been detected by laboratory experiments and field observation [19, 20]. Additionally, Benincà et al. [49] present the first experimental demonstration of chaos in a long-term experiment with a complex food web, where the food web was consisted of bacteria, several phytoplankton species, herbivorous and predatory zooplankton species, and detritivores. And they also find that the community moved back and forth between stabilizing and chaotic dynamics during the cyclic succession, and their findings provide a field demonstration of nonequilibrium coexistence of competing species through a cyclic succession at the edge of chaos [50]. These reports support that the nonequilibrium dynamics, such as oscillations and chaos, can exist in reality.

In the present paper, we find that the unique positive equilibrium may lose its stability via Hopf bifurcation when delay appears, and then a periodic solution emerges, which means that nutrient-phytoplankton oscillation occurs. Obviously, the factor giving rise to nutrient- phytoplankton oscillation is delay in our studies. And the period and the stability of the bifurcating periodic solutions with respect to delay are discussed by using center manifold argument and normal form theory. In fact, instability induced by delay in nutrient-plankton model has been studied widely, and many studies indicate that the equilibrium is always unstable when delay is beyond a critical value [25, 29, 51, 52]. Yet, it should be emphasized in the present paper that the stability switches induced by delay can occur under some conditions.

Moreover, numerical simulations showed how the delay influences nutrient-phytoplankton dynamics. Numerical results for model (1) in the fully nonlinear regime are consistent with the linear analysis. In numerical simulations, we found that delay indeed gives rise to the emergence of stability switches for the positive equilibrium. Yet, the numerical results show that the parameter intervals for stability switches may depend on other parameters as well, e.g., β_2. Additionally, numerical results also indicated that periodic-2 solutions and periodic-3 solutions can emerge under some conditions for delay, which means that complex dynamics induced by delay exist in model (1). From biological viewpoint, the existence of periodic solutions implies that the fluctuations exist in density of phytoplankton population; that is, nutrient-phytoplankton oscillation emerges. Especially, by Li and York's theory, periodic-3 solution implies chaos, which means that chaotic density fluctuations can display a variety of different periodicities and the long-term prediction of phytoplankton density can be fundamentally impossible. The chaotic density fluctuations do not contribute to the control of phytoplankton bloom. Consequently, the importance of the present paper is not the precision with which it predicts specific events for phytoplankton blooms but its contribution to the studies on how the delay influences nutrient-phytoplankton dynamics.

Data Availability

The data used to support the findings of this study are included within the article.

Conflicts of Interest

The author declares that there are no conflicts of interest.

Acknowledgments

This work was supported by the Zhejiang Provincial Natural Science Foundation of China under Grant no. LQ18C030002, the National Natural Science Foundation of China (Grant nos. 61871293, 31570364, and 41876124), and the Zhejiang Provincial Natural Science Foundation of China under Grant no. LY16B070008.

References

[1] J. Huisman, G. A. Codd, H. W. Paerl, B. W. Ibelings, J. M. Verspagen, and P. M. Visser, “Cyanobacterial blooms,” *Nature Reviews Microbiology*, vol. 16, no. 8, pp. 471–483, 2018.

[2] A. Burson, M. Stomp, E. Greenwell, J. Grosse, and J. Huisman, “Competition for nutrients and light: Testing advances in resource competition with a natural phytoplankton community,” *Ecology*, vol. 99, no. 5, pp. 1108–1118, 2018.

[3] M. Stomp, J. Huisman, F. De Jongh, A. J. Veraart, D. Gerla, M. Rijkeboer et al., “Adaptive divergence in pigment composition promotes phytoplankton biodiversity,” *Nature*, vol. 432, no. 7013, pp. 104–107, 2004.

[4] Z. Ma, T. Fang, R. W. Thring et al., “Toxic and non-toxic strains of Microcystis aeruginosa induce temperature dependent allelopathy toward growth and photosynthesis of Chlorella vulgaris,” *Harmful Algae*, vol. 48, pp. 21–29, 2015.

[5] P. W. Boyd, A. J. Watson, C. S. Law et al., “A mesoscale phytoplankton bloom in the polar Southern Ocean stimulated by iron fertilization,” *Nature*, vol. 407, no. 6805, pp. 695–702, 2000.

[6] Z. Ma, H. Yu, R. Thring, C. Dai, A. Shen, and M. Zhao, “Interaction between simulated dense Scenedesmus dimorphus (Chlorophyta) bloom and freshwater meta-zooplankton community,” *Journal of Limnology*, vol. 77, no. 2, pp. 255–263, 2018.

[7] G. Rhee and I. J. Gotham, “The effect of environmental factors on phytoplankton growth: Temperature and the interactions of temperature with nutrient limitation,” *Limnology and Oceanography*, vol. 26, no. 4, pp. 635–648, 1981.

[8] V. H. Smith, “Low nitrogen to phosphorus ratios favor dominance by blue-green algae in lake phytoplankton,” *Science*, vol. 221, no. 4611, pp. 669–671, 1983.

[9] J. A. Downing and E. McCauley, “The nitrogen: Phosphorus relationship in lakes,” *Limnology and Oceanography*, vol. 37, no. 5, pp. 936–945, 1992.

[10] H. Xu, H. W. Paerl, B. Qin, G. Zhu, and G. Gao, “Nitrogen and phosphorus inputs control phytoplankton growth in eutrophic Lake Taihu, China,” *Limnology and Oceanography*, vol. 55, no. 1, pp. 420–432, 2010.

[11] J. H. Ryther and W. M. Dunstan, “Nitrogen, phosphorus, and eutrophication in the coastal marine environment,” *Science*, vol. 171, no. 3975, pp. 1008–1013, 1971.

[12] J. E. Truscott and J. Brindley, “Ocean plankton populations as excitable media,” *Bulletin of Mathematical Biology*, vol. 56, no. 5, pp. 981–998, 1994.

[13] J. A. Freund, S. Mieruch, B. Scholze, K. Wiltshire, and U. Feudel, “Bloom dynamics in a seasonally forced phytoplankton-zooplankton model: Trigger mechanisms and timing effects,” *Ecological Complexity*, vol. 3, no. 2, pp. 129–139, 2006.

[14] T. Zhang and W. Wang, “Hopf bifurcation and bistability of a nutrient-phytoplankton-zooplankton model,” *Applied Mathematical Modelling*, vol. 36, no. 12, pp. 6225–6235, 2012.

[15] A. Huppert, B. Blasius, and L. Stone, “A model of phytoplankton blooms,” *The American Naturalist*, vol. 159, no. 2, pp. 156–171, 2002.

[16] H. Ishii and I. Takagi, “Global stability of stationary solutions to a nonlinear diffusion equation in phytoplankton dynamics,” *Journal of Mathematical Biology*, vol. 16, no. 1, pp. 1–24, 1982.

[17] A. Fan, P. Han, and K. Wang, “Global dynamics of a nutrient-plankton system in the water ecosystem,” *Applied Mathematics and Computation*, vol. 219, no. 15, pp. 8269–8276, 2013.

[18] J. A. Sherratt and M. J. Smith, “Periodic travelling waves in cyclic populations: Field studies and reaction-diffusion models,” *Journal of the Royal Society Interface*, vol. 5, no. 22, pp. 483–505, 2008.

[19] G. F. Fussmann, S. P. Ellner, K. W. Shertzer, and N. G. Hairston Jr., “Crossing the hopf bifurcation in a live predator-prey system,” *Science*, vol. 290, no. 5495, pp. 1358–1360, 2000.

[20] J. Huisman, N. N. Pham Thi, D. M. Karl, and B. Sommeijer, “Reduced mixing generates oscillations and chaos in the oceanic deep chlorophyll maximum,” *Nature*, vol. 439, no. 7074, pp. 322–325, 2006.

[21] Y. Li, Y. Liu, L. Zhao, A. Hastings, and H. Guo, “Exploring change of internal nutrients cycling in a shallow lake: A dynamic nutrient driven phytoplankton model,” *Ecological Modelling*, vol. 313, pp. 137–148, 2015.

[22] B. Liu, H. E. de Swart, and V. N. de Jonge, “Phytoplankton bloom dynamics in turbid, well-mixed estuaries: A model study,” *Estuarine, Coastal and Shelf Science*, vol. 211, pp. 137–151, 2018.

[23] S. G. Ruan, “Persistence and coexistence in zooplankton-phytoplankton-nutrient models with instantaneous nutrient recycling,” *Journal of Mathematical Biology*, vol. 31, no. 6, pp. 633–654, 1993.

[24] J. Caperon, “Time lag in population growth response of isochrysis galbana to a variable nitrate environment,” *Ecology*, vol. 50, no. 2, pp. 188–192, 1969.

[25] J. Zhao and J. Wei, “Dynamics in a diffusive plankton system with delay and toxic substances effect,” *Nonlinear Analysis: Real World Applications*, vol. 22, pp. 66–83, 2015.

[26] S. Ruan and X.-Q. Zhao, “Persistence and extinction in two species reaction-diffusion systems with delays,” *Journal of Differential Equations*, vol. 156, no. 1, pp. 71–92, 1999.

[27] Y. Wang, W. Jiang, and H. Wang, “Stability and global Hopf bifurcation in toxic phytoplankton-zooplankton model with delay and selective harvesting,” *Nonlinear Dynamics*, vol. 73, no. 1-2, pp. 881–896, 2013.

[28] C. Dai, M. Zhao, H. Yu, and Y. Wang, “Delay-induced instability in a nutrient-phytoplankton system with flow,” *Physical Review E: Statistical, Nonlinear, and Soft Matter Physics*, vol. 91, no. 3, p. 032929, 2015.

[29] C. Dai, M. Zhao, and H. Yu, "Dynamics induced by delay in a nutrient-phytoplankton model with diffusion," *Ecological Complexity*, vol. 26, pp. 29–36, 2016.

[30] K. Chakraborty, K. Das, and T. K. Kar, "Modeling and analysis of a marine plankton system with nutrient recycling and diffusion," *Complexity*, vol. 21, no. 1, pp. 229–241, 2015.

[31] V. Volterra, *Lecons Sur La Théorie Mathématique De La Lutte Par La Vie*, Gauthier-Villars, Paris, 1931.

[32] J. K. Hale and L. Verduyn, *Theory of Functional Differential Equations*, Springer, New York, NY, USA, 1993.

[33] Y. Kuang, *Delay differential equations with applications in population dynamics*, Academic Press, Boston, Mass, USA, 1993.

[34] J. Wu, *Theory and Applications of Partial Functional Differential Equations*, Springer, New York, NY, USA, 1996.

[35] S. Gakkhar and A. Singh, "Complex dynamics in a prey predator system with multiple delays," *Communications in Nonlinear Science and Numerical Simulation*, vol. 17, no. 2, pp. 914–929, 2012.

[36] N. MacDonald, "Time delay in prey-predator models," *Mathematical Biosciences*, vol. 28, no. 3-4, pp. 321–330, 1976.

[37] S. Ruan and J. Wei, "On the zeros of transcendental function with applications to stability of delay differential equations with two zeros," *Dynamics of Continuous, Discrete and Impulsive Systems Series A: Mathematical Analysis*, vol. 10, pp. 863–874, 2003.

[38] C. Xu, "Delay-induced oscillations in a competitor-competitor-mutualist lotka-volterra model," *Complexity*, vol. 2017, Article ID 2578043, 12 pages, 2017.

[39] S. S. Chen and J. J. Wei, "Stability and bifurcation in a diffusive logistic population model with multiple delays," *International Journal of Bifurcation & Chaos*, vol. 25, no. 8, p. 1550107, 2015.

[40] K. Wang, W. Wang, H. Pang, and X. Liu, "Complex dynamic behavior in a viral model with delayed immune response," *Physica D: Nonlinear Phenomena*, vol. 226, no. 2, pp. 197–208, 2007.

[41] Y. Song, J. Wei, and Y. Yuan, "Stability switches and Hopf bifurcations in a pair of delay-coupled oscillators," *Journal of Nonlinear Science*, vol. 17, no. 2, pp. 145–166, 2007.

[42] S. Chen, Y. Lou, and J. Wei, "Hopf bifurcation in a delayed reaction- diffusion-advection population model," *Journal of Differential Equations*, vol. 264, no. 8, pp. 5333–5359, 2018.

[43] B. D. Hassard, N. D. Kazarinoff, and Y.-H. Wan, *Theory and Applications of Hopf Bifurcation*, Cambridge University Press, Cambridge, UK, 1981.

[44] Y. Song and J. Wei, "Bifurcation analysis for Chen's system with delayed feedback and its application to control of chaos," *Chaos, Solitons & Fractals*, vol. 22, no. 1, pp. 75–91, 2004.

[45] J. Guckenheimer and P. Holmes, *Nonlinear Oscillations, Dynamical Systems, and Bifurcation of Vector Fields*, Springer-Verlag, New York, NY, USA, 1983.

[46] Y. Kuang, *Delay Differential Equations with Applications in Population Dynamics*, Academic Press, New York, NY, USA, 1993.

[47] A. F. Nindjin, M. A. Aziz-Alaoui, and M. Cadivel, "Analysis of a predator-prey model with modified Leslie-Gower and Holling-type II schemes with time delay," *Nonlinear Analysis: Real World Applications*, vol. 7, no. 5, pp. 1104–1118, 2006.

[48] Y. Deng, M. Zhao, H. Yu, and Y. Wang, "Dynamical analysis of a nitrogen-phosphorus-phytoplankton model," *Discrete Dynamics in Nature and Society*, vol. 2015, Article ID 823026, 8 pages, 2015.

[49] E. Benincá, J. Huisman, R. Heerkloss et al., "Chaos in a long-term experiment with a plankton community," *Nature*, vol. 451, no. 7180, pp. 822–825, 2008.

[50] E. Benincà, B. Ballantine, S. P. Ellner, and J. Huisman, "Species fluctuations sustained by a cyclic succession at the edge of chaos," *Proceedings of the National Acadamy of Sciences of the United States of America*, vol. 112, no. 20, pp. 6389–6394, 2015.

[51] K. Das and S. Ray, "Effect of delay on nutrient cycling in phytoplankton-zooplankton interactions in estuarine system," *Ecological Modelling*, vol. 215, no. 1-3, pp. 69–76, 2008.

[52] H. Zhao, X. Huang, and X. Zhang, "Hopf bifurcation and harvesting control of a bioeconomic plankton model with delay and diffusion terms," *Physica A: Statistical Mechanics and its Applications*, vol. 421, pp. 300–315, 2015.

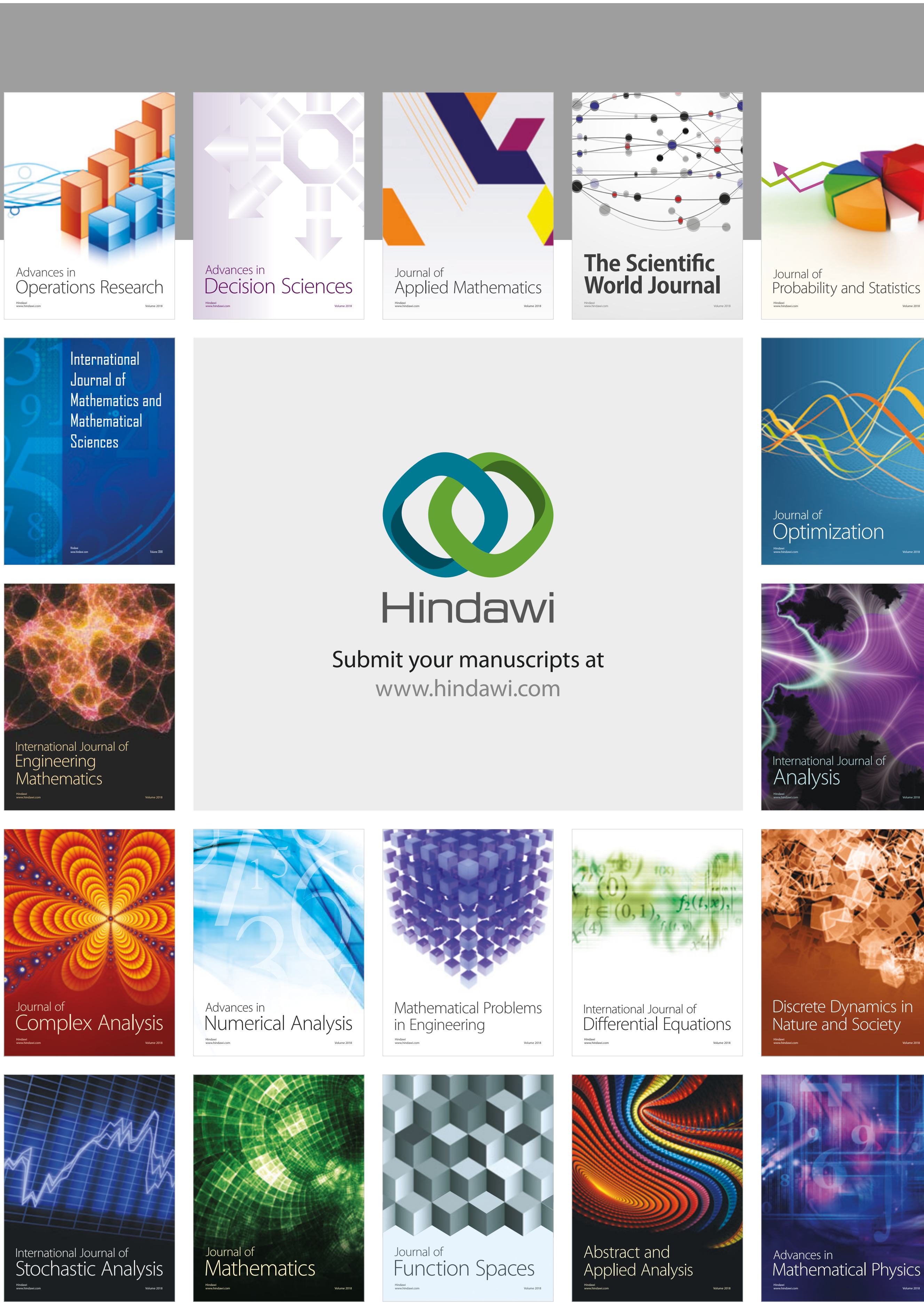

Advances in Operations Research
Advances in Decision Sciences
Journal of Applied Mathematics
The Scientific World Journal
Journal of Probability and Statistics
International Journal of Mathematics and Mathematical Sciences
Hindawi
Submit your manuscripts at
www.hindawi.com
Journal of Optimization
International Journal of Engineering Mathematics
International Journal of Analysis
Journal of Complex Analysis
Advances in Numerical Analysis
Mathematical Problems in Engineering
International Journal of Differential Equations
Discrete Dynamics in Nature and Society
International Journal of Stochastic Analysis
Journal of Mathematics
Journal of Function Spaces
Abstract and Applied Analysis
Advances in Mathematical Physics